NACA

RESEARCH MEMORANDUM

INVESTIGATION OF TRANSLATING-DOUBLE-CONE AXISYMMETRIC INLETS WITH COWL PROJECTED AREAS 40 AND 20 PERCENT OF MAXIMUM AT MACH NUMBERS FROM 3.0 TO 2.0

By James F. Connors, George A. Wise, and J. Calvin Lovell

Lewis Flight Propulsion Laboratory
Cleveland, Ohio

NATIONAL ADVISORY COMMITTEE
FOR AERONAUTICS

WASHINGTON

May 20, 1957

NACA RM E57C06

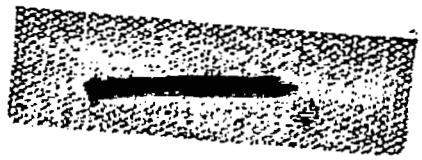

NATIONAL ADVISORY COMMITTEE FOR AERONAUTICS

RESEARCH MEMORANDUM

INVESTIGATION OF TRANSLATING-DOUBLE-CONE AXISYMMETRIC INLETS WITH COWL PROJECTED AREAS 40 AND 20 PERCENT OF MAXIMUM AT MACH NUMBERS FROM 3.0 TO 2.0

By James F. Connors, George A. Wise, and J. Calvin Lovell

SUMMARY

The performance of two translating-double-cone inlets with contrasting rates of turning on the spike shoulder and corresponding cowl projected frontal areas of 40 and 20 percent of maximum was compared over the Mach number range from 3.0 to 2.0. Pressure recoveries were about the same for both configurations, the 20-percent-cowl inlet falling 0.01 to 0.03 lower than the 40-percent-cowl inlet over the entire range of Mach number and angle of attack up to 15°. At Mach 3.01, the 20-percent-cowl inlet had a recovery of 0.625 compared with 0.635 for the 40-percent-cowl inlet. At this same Mach number, the cowl pressure-drag coefficient for the 20-percent cowl (0.103 based on max. projected model frontal area) was 45 percent less than that for the 40-percent cowl (0.187). On a propulsive-thrust basis, the 20-percent-cowl inlet was superior over the entire range of Mach number.

Total and component drags were obtained at Mach numbers 3.01, 2.73, 2.44, and 1.97. In order to match the airflow requirements of a hypothetical turbojet engine, the second oblique shock was located at the cowl lip at each Mach number. Total drag coefficients during supercritical inlet operation increased with decreasing Mach number, primarily because of the increasing additive drags. Distortions at zero angle of attack were low, about 0.02 at Mach 3.01 and about 0.12 at Mach 1.97.

With the 40-percent-cowl inlet, retracting the spike slightly from its design position at Mach 3.01 resulted in a stable subcritical range of mass-flow ratio from 1.0 to 0.6. This result did not occur with the 20-percent-cowl inlet.

INTRODUCTION

Currently, there is a scarcity of detailed performance data on inlets suitable for application to turbojet engines operating to Mach

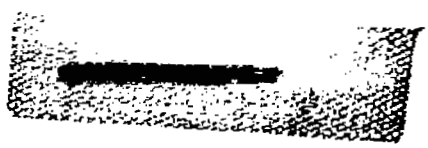

numbers of approximately 3.0. For wide-range variable Mach number operation, variable-geometry features appear necessary to maintain high performance levels. For such inlets, information is needed to ascertain the "on- and off-design" pressure-recovery and drag characteristics and their interrelation on a propulsive-thrust basis.

The objective of the present study was to evaluate the performance of translating-double-cone axisymmetric nose inlets designed to match the airflow requirements of a hypothetical turbojet engine up to a Mach number of 3.0. Two versions, both utilizing 20°-35° double-cone spikes, were designed with two different objectives in mind: (1) good internal performance and (2) good external performance or low drag. The purpose was to determine partially the balance between drag and pressure recovery. The first version had a gradual turn at the shoulder of the spike which necessitated a cowl with a projected frontal area equal to 40 percent of maximum. The other version, with a more rapid turn at the spike shoulder, had a cowl with a projected area 20 percent of maximum.

The geometry of these inlets was such that both oblique shocks coalesced at the cowl lip at a Mach number of 3.0. At the lower Mach numbers the airflow requirements of the engine could be satisfied by maintaining the second oblique shock at the cowl lip. Data were also obtained for off-design spike positions at a Mach number of 3.0.

These data should indicate the performance levels attainable with inlets of rather basic and conventional design. As such, they should serve as a base of reference with which to compare the performance of other configurations employing additional refinements such as boundary-layer control or geometry variations.

The present investigation was performed in the NACA Lewis 10- by 10-foot supersonic wind tunnel at Mach numbers of 3.01, 2.73, 2.44, and 1.97 and at angles of attack to 15°. Reynolds number of the test was constant at 2.5×10^{6} per foot.

SYMBOLS

A	area, sq ft
A_{in}	inlet capture area, 1.182 sq ft
A_{max}	maximum projected frontal area of model, 1.973 sq ft for 40-percent cowl and 1.483 sq ft for 20-percent cowl
A_x	area normal to flow direction in duct, sq in.

[redacted]

A_3	diffuser-exit flow area, 0.961 sq ft
C_D	drag coefficient, D/q_0A_{max}
$C_{D,c}$	cowl pressure-drag coefficient, $\frac{1}{y_{max}^2}\int_{y_l}^{y_{max}} C_p \, dy^2$
C_p	static-pressure coefficient, $(p - p_0)/q_0$
D	drag, lb
D_{c+a}	cowl pressure drag plus additive drag
F	thrust, lb
F_{id}	ideal thrust; i.e., F at $\overline{P}_3/P_0 = 1.0$
$\frac{F - D_{c+a}}{F_{id}}$	thrust parameter
M	Mach number
m_3/m_0	inlet mass-flow ratio, $\rho_3V_3A_3/\rho_0V_0A_{in}$
$\Delta m_3/m_0$	stable subcritical operating range
P	total pressure, lb/sq ft
$\overline{P}_3/P_0$	total-pressure recovery
$\frac{P_{3,max} - P_{3,min}}{\overline{P}_3}$	flow-distortion parameter
p	static pressure, lb/sq ft
q	dynamic pressure, lb/sq ft
V	air velocity, ft/sec
w	weight flow, lb/sec
$\frac{w_3\sqrt{\theta_3}}{\delta_3A_3}$	corrected weight flow at station 3, (lb/sec)/sq ft
x	distance along axis of symmetry

y	distance from axis of symmetry
α	angle of attack, deg
δ_3	ratio of total pressure at station 3 to NACA standard sea-level pressure of 2116 lb/sq ft
θ_l	cowl-position parameter, angle between axis of symmetry and line from spike tip to cowl lip, deg
θ_3	ratio of total temperature at station 3 to NACA standard sea-level temperature of 518.7° R
ρ	density of air, lb/cu ft

Subscripts:

e	external
l	lip
max	maximum
min	minimum
0	conditions in free stream
3	conditions at diffuser exit

Superscript:

$\bar{}$	area-weighted value

APPARATUS AND PROCEDURE

Schematic drawings of the over-all model and the inlets are presented in figures 1(a) and (b), respectively. A photograph of the model in the tunnel is shown in figure 1(c). The model was sting-mounted in the tunnel through a three-component strain-gage balance, and a movable exit plug was mounted on the sting independently of the model in order to vary the inlet back pressure. Provisions were made for including interchangeable liners at the duct exit (fig. 1(a)) in order to decrease the net axial forces at the higher Mach numbers and remain within the range of the balance. The model also incorporated provisions for changing spikes and cowls and for translating the spike by remote control.

The inlet had a 20°-35° double-cone spike designed so that the two oblique shocks would coalesce at the cowl lip at a Mach number of 3.0. Two modifications of this spike, having different rates of turning at the shoulder, were tested (fig. 1(b) and tables I and II). The sharper of the two turning rates resulted in a cowl with a projected frontal area equal to 20 percent of maximum; the cowl for the more gradual turn had a projected frontal area 40 percent of maximum. Turning of the flow from the inlet back to the axial direction at Mach 3.01 was effected in approximately 3 hydraulic diameters with the 40-percent cowl and in about 1 hydraulic diameter with the 20-percent cowl. The initial lip angles, however, were the same for both cowls: external angle 32.6° and internal angle 27.6°, referenced to the axis of symmetry.

Internal area distributions are presented in figure 2. The form of these distributions was influenced to a great extent by an attempt to avoid internal contraction as the spike was retracted. Generally, the more gradual the rate of internal area expansion at the higher Mach number, the more quickly internal contraction will be incurred at the lower Mach numbers. At the design spike position for a Mach number of 3.01, the initial equivalent conical area expansion corresponded to a 15° included angle for the 40-percent cowl and approximately 42° for the 20-percent cowl. Both inlets had some internal contraction when the spike was retracted to the design position for a Mach number of 1.97.

Pressure recovery was determined from an area-weighted average of 48 total-pressure tubes at station 3 (fig. 1(a)). Mass-flow ratio m_3/m_0 was based on the mass flow computed from six static pressures at station 3 and the measured sonic discharge area, assuming one-dimensional isentropic flow. This mass-flow measuring technique was calibrated by means of an inlet capturing a known free-stream tube of air.

Cowl pressure drag was determined from an integration of the experimental pressure distributions. External drag was defined as the difference between the axial force given by the balance and the internal thrust obtained from the total momentum change between the inlet and the sonic exit station (including the model base forces and excluding the forces on the movable plug). Friction drag was obtained by subtracting the cowl pressure drag from the total external drag in the case of no spillage (or additive) drag. The order of magnitude of this friction drag was verified by a momentum integration of an experimental boundary-layer profile obtained with the 40-percent-cowl inlet. Another order-of-magnitude check was obtained with the von Kármán skin-friction coefficient (≈ 0.0015) for turbulent boundary layer on a flat plate at a Mach number of 3.0. In cases of subcritical inlet operation, additive drag was approximated by assuming the friction drag to be the same as for the no-spillage case and then subtracting the sum of the cowl pressure and friction drags from the total external drags.

The investigation was conducted at Mach numbers of 3.01, 2.73, 2.44, and 1.97 and through an angle-of-attack range of 0° to 15°. Reynolds number of the test was held constant at 2.5×10^6 per foot.

RESULTS AND DISCUSSION

The two double-cone inlets with their contrasting rates of turning had different design objectives: The 40-percent-cowl inlet was aimed at high recovery; the 20-percent-cowl inlet, at low drag. For comparison purposes, parallel presentations are made of the performance of these two inlets. Detailed results are subdivided into sections on internal-flow performance (pressure-recovery and mass-flow characteristics), external-flow performance (drags), inlet airflow patterns, and finally a propulsive-thrust comparison.

Internal-Flow Performance

Diffuser characteristics at design spike positions. - Total-pressure-recovery and mass-flow characteristics for the two inlets at their design values of cowl-position parameter θ_l are presented in figure 3. At each Mach number, the spike position was determined for the zero-angle-of-attack condition (second oblique shock on lip) and then held constant for the range of angles (α) investigated. A cross plot (fig. 4) summarizes the variation in critical inlet performance with free-stream Mach number.

Both inlets achieved essentially the same level of internal performance. The 20-percent-cowl inlet with the much sharper turning showed only a slight decrease in pressure recovery, a decrement of approximately 0.01 to 0.03 below that for the 40-percent-cowl inlet over the entire range of Mach number. At $M_0 = 3.01$ the 20-percent-cowl inlet attained a pressure recovery of 0.625 compared with 0.635 for the 40-percent cowl. Airflow capacities, as reflected in mass-flow ratio and corrected airflow, were about the same for both inlets. At zero angle of attack, the 20-percent-cowl inlet consistently had a larger stable subcritical range than the 40-percent-cowl inlet. The rapid decrease in mass-flow ratio at Mach numbers less than approximately 2.2 was the result of detached-shock operation, caused by the large cowl-lip angles or by internal choking. Above this Mach number, supercritical spillage occurred only behind the first conical shock, as dictated by the design requirement that the second shock be located at the cowl lip.

Effect of angle of attack. - As shown in figure 5, both critical pressure recovery and mass-flow ratio decreased with angle of attack. The rate of decrease was about the same for both inlets and for each

Mach number investigated. The pressure recovery of the 20-percent-cowl inlet remained consistently lower by a small amount (0.01 to 0.03) than that of the 40-percent-cowl inlet.

Effect of cowl-position parameter at Mach 3.01 and zero angle of attack. - Diffuser performance curves for both inlets at several different spike positions at $M_0 = 3.01$ are shown in figure 6. These data and the cross plots of figure 7 illustrate the effect of θ_l on subcritical inlet stability. By retracting the spike to increase θ_l about 0.6° above the design value, the 40-percent-cowl inlet achieved quite a large stable range of mass-flow ratio, from 1.0 down to approximately 0.6. This, however, was at the expense of a decrease in critical pressure recovery from 0.635 to 0.585. This scheme, possibly, could serve as a convenient method for reduced-mass-flow operation in a turbojet application. Previously, similar results had been obtained with axisymmetric inlets at lower Mach numbers (e.g., at $M_0 = 2$ in ref. 1). By placing the oblique shocks just inside the cowl, the slipline during subcritical operation (ref. 2) does not intercept the cowl lip, and the associated buzz-triggering mechanism is avoided.

Similar results did not occur with the 20-percent-cowl configuration. On the contrary, when θ_l was increased above the design value, the subcritical stable range actually decreased from the 0.15 to 0.17 range available with the oblique shocks on or slightly ahead of the cowl lip. These diverse results may be attributed to the difference between the two inlets in internal area expansion at the centerbody shoulder. Presumably, the 20-percent-cowl inlet had an internal geometry more conducive to flow separation and choking of the duct than the more gradually divergent passage of the 40-percent-cowl configuration. Subsequent tests (not yet reported) substantiate these observations.

Total-pressure variations at diffuser exit. - Total-pressure profiles at the diffuser exit for several angles of attack are presented in figure 8 in the form of contour maps. The $M_0 = 3.01$ condition shown is typical for the entire Mach number range. Similar results were obtained with both the 40- and the 20-percent-cowl inlets. At zero angle of attack, the flow was quite uniform. With increasing angle of attack, the high-energy air shifted to the upper quadrant of the duct, while separation occurred in the lower quadrant.

The usual distortion parameter $(P_{3,max} - P_{3,min})/\overline{P}_3$ was employed as a measure of nonuniformity of the flow at the diffuser exit. The variation in distortion level with angle of attack during critical inlet operation is presented in figure 9 for the four Mach numbers investigated. At each Mach number the distortion was a minimum at zero and increased rapidly with increasing angle of attack. At $M_0 = 1.97$ with detached-shock operation, the rate of increase in distortion was less than that

at the three higher Mach numbers. Distortion at angle of attack was generally higher with the 20- than with the 40-percent-cowl inlet. At $M_0 = 3.01$, distortion ranged from 0.02 at $\alpha = 0°$ to 0.40 at $\alpha = 15°$ for the 40-percent-cowl inlet.

The zero-angle-of-attack distortion during critical inlet operation increased with decreasing free-stream Mach number and concomitantly with increasing diffuser-exit Mach number. This observation is shown in figure 10, along with a comparison of the experimental distortion levels with theoretical values for 1/7-power fully developed pipe flow (ref. 3). Both inlets had slightly lower distortion at $M_0 = 3.01$ and 2.73 than the pipe-flow values and somewhat higher values at the lower free-stream Mach numbers. Zero-angle-of-attack distortions varied from 0.02 at Mach 3.01 to 0.125 at Mach 1.97.

External-Flow Performance

Supercritical cowl pressure drags. - External static-pressure distributions along the cowl of each inlet during supercritical operation at Mach 3.01 and zero angle of attack are presented in figure 11. Distributions based on two-dimensional shock-expansion theory are also included for comparison purposes. With the 20-percent cowl, there was good agreement between experiment and theory; with the 40-percent cowl, the agreement was not so good, with shock-expansion theory generally overestimating the pressures. The greater discrepancy between experiment and theory encountered with the 40-percent cowl can be attributed to the greater variation in radius (a larger three-dimensional effect) than with the 20-percent cowl. At below design Mach number (3.0), an approximation of the initial conical flow field was made to obtain the local flow condition at the cowl lip with the first oblique shock out in front. This approximation was the assumption of a linear variation of Mach number and flow angle between the shock and the cone surface.

Based on area integrations of the static-pressure distributions, cowl pressure-drag coefficients are shown in figure 12 for the entire Mach number range. The cowl pressure drags for the two inlets were significantly different. At $M_0 = 3.01$, the cowl drag coefficient for the 20-percent cowl was 45 percent less than that for the 40-percent cowl. At $M_0 = 3.01$, the drag coefficient (based on max. frontal area) for the 40-percent cowl was 0.187, compared with a drag coefficient of 0.103 for the 20-percent-cowl inlet. The cowl pressure-drag coefficients increased slightly with decreasing Mach number until shock detachment occurred, after which there was a slight decrease.

Drags obtained from integration of pressure distributions based on shock-expansion theory are also included in figure 12. Agreement between

experiment and theory was generally good over the range of Mach number investigated. The greatest discrepancy occurred at $M_0 = 3.01$ with the 40-percent cowl, where the difference amounted to 10 percent of the experimental value.

External-drag components. - For supercritical inlet operation, the variation in total external drag and its components with free-stream Mach number is shown in figure 13. Total external drags derived from actual force measurements agreed reasonably well with those given by summation of the component drags (cowl pressure, additive, and friction). In this case a computed additive drag was used in the summation. The total external-drag coefficients for maximum mass flow and design θ_l increased with decreasing free-stream Mach number, primarily as a consequence of increasing supercritical additive drags. The difference in total drags between the 40- and 20-percent-cowl inlets is essentially the difference in their respective cowl pressure drags.

During subcritical inlet operation (such as that illustrated in fig. 14), there is a large linear increase in external drag with decreasing mass-flow ratio as a result of the high additive drags associated with bow-shock spillage. Also with reduced mass flows, there is a reduction in cowl pressure drag. Assuming friction constant with mass-flow ratio, rough momentum calculations verified the order of magnitude of the additive drag at the minimum stable condition.

The subcritical total-drag rise $\Delta C_{D,e}/(\Delta m_3/m_0)$ is given in figure 15 for the range of test conditions under which stability was achieved. The rate of subcritical drag rise, particularly for the 40-percent-cowl inlet, did not vary significantly with Mach number. The pronounced difference between the two inlets is attributed to a difference in the rate of decrease in cowl pressure drag with mass flow. Presumably, the 40-percent cowl with its larger projected area was more favorably affected in the direction of leading-edge suction, as the normal shock moved ahead of the lip. Instrumentation in this study was inadequate near the cowl lip to define this effect fully.

Inlet Airflow Patterns

Supercritical operation at design cowl-position parameter. - Supercritical inlet airflow patterns at zero angle of attack are shown in figure 16 for both inlets at each of the four Mach numbers investigated. At this Reynolds number (2.5×10^6 per ft), there was little or no bridging due to boundary-layer separation at the break between the cones. At Mach 3.01, both oblique shocks appeared to coalesce at the cowl lip. As Mach number was reduced, the second oblique shock was maintained at the lip and the first oblique moved progressively farther upstream of the

cowl, until shock detachment at the lip occurred, as is shown for $M_0 = 1.97$. Supercritical patterns for both the 40- and 20-percent-cowl inlets at several angles of attack at Mach 3.01 are shown in figure 17. Shock patterns are generally conventional, with detachment at the bottom cowl lip occurring at the higher angles and the initial conical shock on top moving progressively farther ahead of the lip with increasing angle of attack.

40-Percent-cowl inlet at M_0 of 3.01 and $\theta_l >$ design. - Schlieren photographs of the 40-percent-cowl inlet at Mach 3.01 and θ_l greater than design are presented in figure 18 for supercritical and minimum stable mass-flow conditions. The spike was retracted from the design position (θ_l approx. $1/2^\circ >$ design) to place both oblique shocks just inside the cowl, as shown in the left photograph. By so doing, a large stable subcritical operating range was attained. The resulting minimum stable mass-flow condition is shown in the right photograph of figure 18. Because of the high degree of resolution in the schlieren system, the lobes of the Kármán vortex street are fairly well defined, with the vertical lines (three-dimensional projections) identifying the spacing between individual vortices. The outer slipline emanating from the intersection of the first oblique and the bow shocks is so curved as to indicate a flow direction in towards the axis immediately behind the bow shock. An inner slipline was formed at the intersection of the bow and the second oblique shocks. Between these inner and outer sliplines, a contracting channel appeared to exist and thus indicated the presence of an accelerating subsonic flow field with an attendant favorable pressure gradient.

This stable flow condition is particularly interesting, because at a free-stream Mach number of 3.01 the local surface Mach number was calculated to be 1.67, a value far in excess of that indicated for a normal shock to separate a turbulent boundary layer (ref. 4). Although separation may exist locally in the zone of interaction, the boundary layer downstream of this zone appears to reattach and follow the surface contour back into the inlet. Similar observations had been made previously with a two-dimensional ramp-type inlet at this Mach number (ref. 5).

Propulsive-Thrust Comparison

The 40- and 20-percent-cowl inlets were compared on the basis of zero-angle-of-attack propulsive thrust, or simply thrust minus drag. Results are shown in figure 19 in terms of a thrust parameter, the ratio of internal thrust minus the sum of cowl pressure plus additive drags to an ideal thrust based on 100-percent pressure recovery. With the inlets matched at the critical condition for all Mach numbers, a turbojet engine with afterburning to 3500° R was assumed in the comparison. The

method of reference 6 was used in the calculations. The dashed lines in figure 19 show the effects of pressure recovery, or the difference in thrust between an inlet attaining 100-percent recovery and the test inlets with their experimental recoveries, assuming no external drag ($D_{c+a} = 0$).

Both inlets achieved about the same level of internal performance and at $M_0 = 3.01$ the maximum possible thrust with no drag is only about 0.57 of ideal thrust. When external drag is taken into account, as illustrated by the solid lines in figure 19, the 20-percent-cowl inlet is definitely superior to the 40-percent-cowl inlet for the entire range of Mach number investigated. At Mach 3.01, this superiority amounts to a 14-percent gain in propulsive thrust for the 20-percent-cowl inlet. Cowl pressure drag, alone, amounted to 22 percent of engine thrust at $M_0 = 3.01$ for the 40-percent-cowl inlet, and about 10 percent for the 20-percent-cowl inlet. Even so, it appears that the major gains in overall thrust performance will lie in the direction of improved pressure recovery.

4405

CQ-2 back

SUMMARY OF RESULTS

Two axisymmetric translating-double-cone inlets, with contrasting rates of turning at the shoulder resulting in cowl projected areas of 40 and 20 percent of maximum frontal area, were experimentally evaluated at Mach numbers from 3.0 to 2.0 in the 10- by 10-foot Lewis unitary wind tunnel. The inlet-engine matching scheme used herein called for the second oblique shock to be located at the cowl lip at all Mach numbers. The following results were obtained:

1. The 20-percent-cowl inlet achieved pressure recoveries only slightly lower (0.01 to 0.03) than the 40-percent-cowl inlet over the entire Mach number range. At Mach 3.01, the 20-percent-cowl inlet had a recovery of 0.625 compared with 0.635 for the 40-percent-cowl configuration.

2. At Mach number 3.01, the cowl pressure-drag coefficient for the 20-percent-cowl inlet (0.103 based on max. frontal area) was only 55 percent of that for the 40-percent-cowl inlet (0.187). On a propulsive-thrust basis, the 20-percent-cowl inlet was markedly superior over the entire Mach number range. Total external-drag coefficients during supercritical inlet operation increased with decreasing Mach number, primarily because of the increasing additive drag.

3. Zero-angle-of-attack distortions during critical operation were low at all Mach numbers, about 0.02 at Mach 3.01 and about 0.12 at Mach 1.97. Distortion increased rapidly with angle of attack (approx. 0.40 at 15° angle of attack at Mach 3.01).

4. With the 40-percent-cowl inlet, increasing cowl-position parameter about 0.6° above the design value at Mach 3.01 resulted in a subcritical stable mass-flow-ratio range from 1.0 to about 0.6. This result did not occur with the 20-percent-cowl inlet.

Lewis Flight Propulsion Laboratory
National Advisory Committee for Aeronautics
Cleveland, Ohio, March 6, 1957

REFERENCES

1. Gorton, Gerald C.: Investigation at Supersonic Speeds of a Translating-Spike Inlet Employing a Steep-Lip Cowl. NACA RM E54G29, 1954.

2. Ferri, Antonio, and Nucci, Louis M.: The Origin of Aerodynamic Instability of Supersonic Inlets at Subcritical Conditions. NACA RM L50K30, 1951.

3. Sterbentz, William H.: Factors Controlling Air-Inlet Flow Distortions. NACA RM E56A30, 1956.

4. Nussdorfer, T. J.: Some Observations of Shock-Induced Turbulent Separation on Supersonic Diffusers. NACA RM E51L26, 1954.

5. Woollett, Richard R., and Connors, James F.: Zero-Angle-of-Attack Performance of Two-Dimensional Inlets Near Mach Number 3. NACA RM E55K01, 1956.

6. Weber, Richard J., and Luidens, Roger W.: A Simplified Method for Evaluating Jet-Propulsion-System Components in Terms of Airplane Performance. NACA RM E56J26, 1956.

[redacted]

4405

TABLE I. - COWL COORDINATES

(a) 40-Percent cowl

Distance from cowl lip, in.	Diameter, in.	
	Internal	External
0.01	14.730	14.770
.50	------	15.376
1.00	15.770	15.980
1.50	16.236	16.474
2.00	16.600	16.894
2.50	16.888	17.264
3.00	17.124	17.540
4.00	17.484	17.944
5.00	17.736	18.246
6.00	17.906	18.464
7.00	18.020	18.600
8.00	18.096	18.688
9.00	18.150	18.760
10.00	18.184	18.820
11.00	18.216	18.868
12.00	18.240	18.918
13.00	18.270	18.956
13.50	18.280	------
14.00	18.292	18.980
15.00	18.300	19.000
16.00	18.280	------
17.00	18.212	------
18.00	18.128	------
19.00	18.040	------
20.00	17.944	------
21.00	17.854	------
22.00	17.760	------
22.50	17.720	------

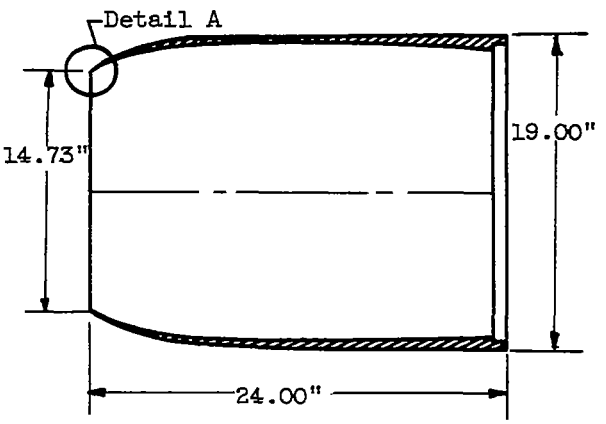

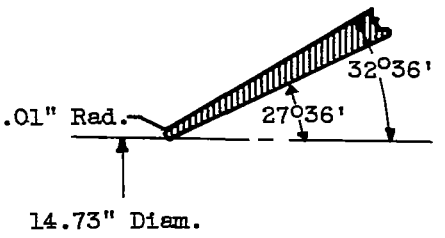

Detail A

TABLE I. - Concluded. COWL COORDINATES

(b) 20-Percent cowl

Distance from cowl lip, in.	Diameter, in.	
	Internal	External
0.01	14.730	14.77
.50	------	15.384
.60	15.344	------
.80	15.514	15.690
1.10	15.700	15.896
1.40	15.840	16.052
1.80	15.964	16.184
2.20	16.044	16.270
2.60	16.100	16.310
3.00	16.140	16.350
3.50	16.174	16.384
4.50	16.190	16.400
5.00	16.200	16.436
6.00	16.210	16.460
7.00	16.200	------
8.00	16.180	------
9.00	16.160	------
10.00	16.150	------
11.00	16.130	------
12.00	16.110	------
13.00	16.064	------
14.00	16.024	------
15.00	15.984	------
16.00	15.944	------
17.00	15.904	------
18.00	15.864	------
19.00	15.820	------
20.00	15.780	------
21.00	15.740	------
22.00	15.700	------
22.50	15.680	16.460

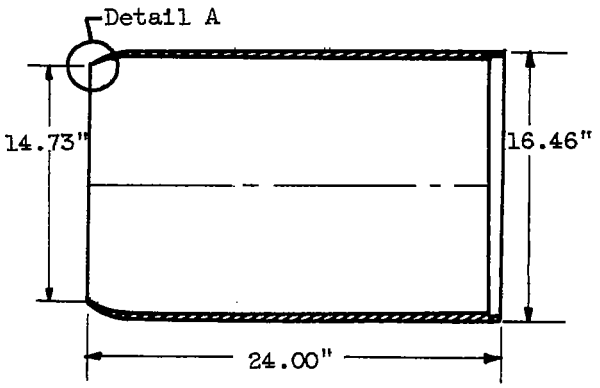

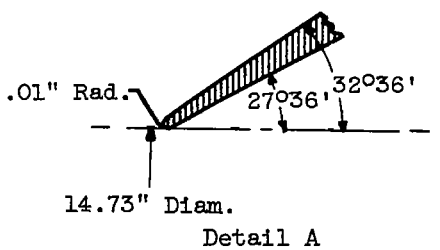

Detail A

[redacted]

4405

TABLE II. - SPIKE COORDINATES

(a) Spike with 40-percent cowl

x, in.	y, in.	
0	0	Straight (20°)
10.50	3.82	
11.30	4.376	Straight (35°)
13.72	6.069	
14.72	6.642	
15.72	6.972	
17.72	7.265	
18.72	7.331	
19.72	7.360	
20.72	7.380	
24.72	7.380	

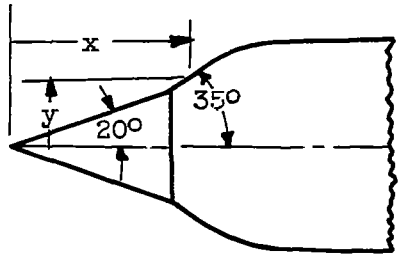

(b) Spike with 20-percent cowl

x, in.	y, in.	
0	0	Straight (20°)
10.50	3.82	
11.30	4.376	Straight (35°)
13.65	6.027	
13.91	6.165	
14.21	6.220	
14.71	6.246	
15.71	6.280	
16.81	6.300	
18.41	6.265	
19.71	6.228	
21.21	6.190	
22.71	6.150	
24.71	6.105	
26.21	6.060	

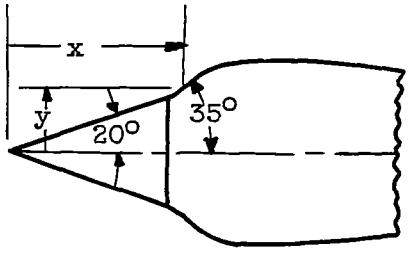

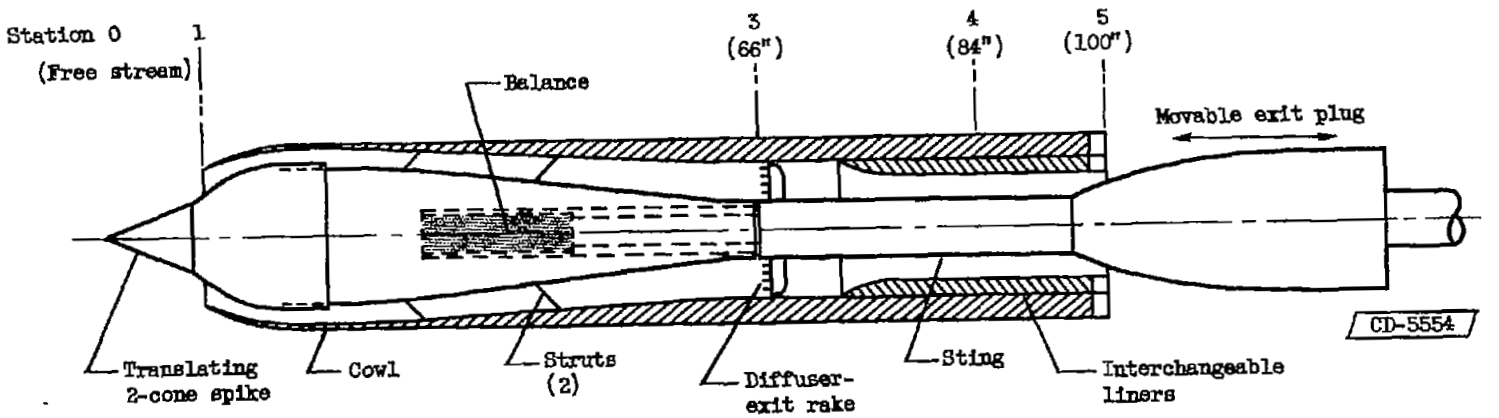

(a) Schematic diagram of over-all test model.

Figure 1. - Experimental apparatus.

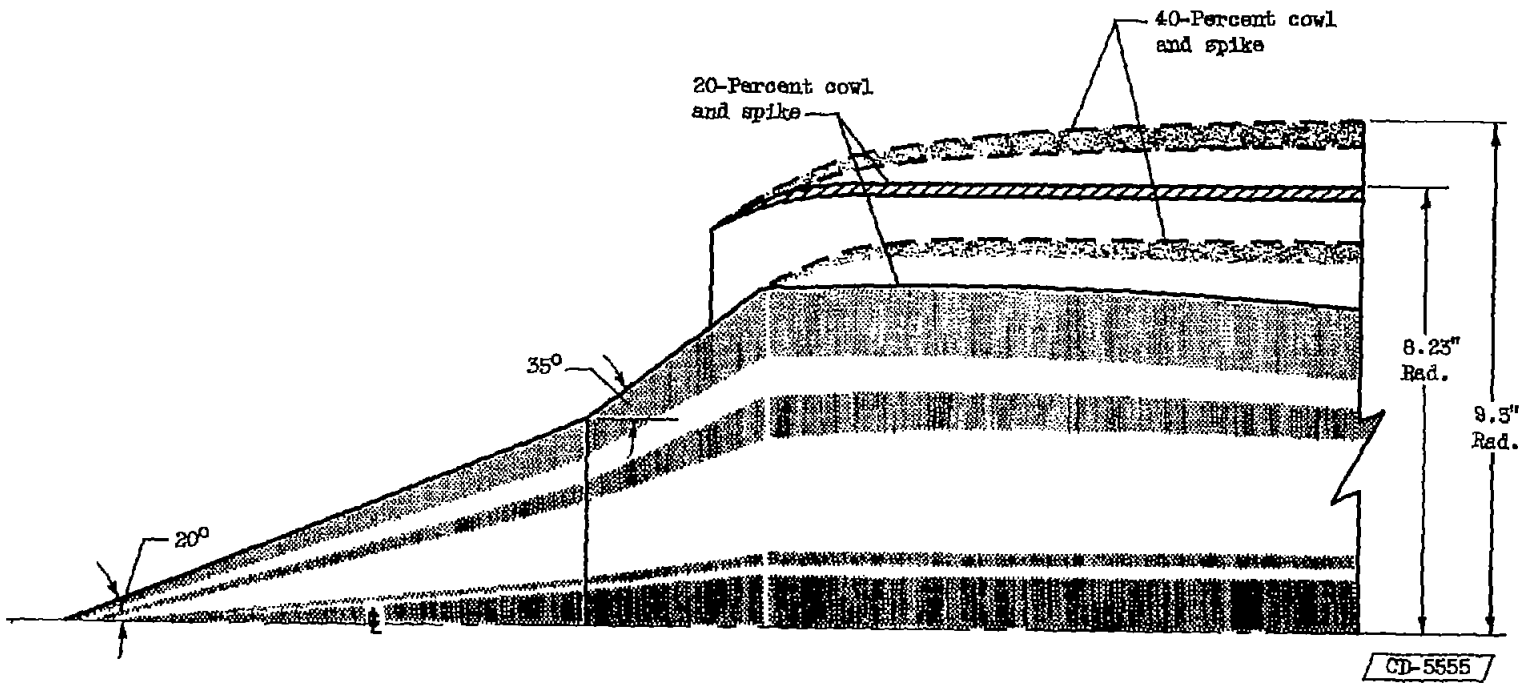

(b) Sketch of the two inlets superimposed.

Figure 1. - Continued. Experimental apparatus.

(c) Test model installed in 10- by 10-foot tunnel.

Figure 1. - Concluded. Experimental apparatus.

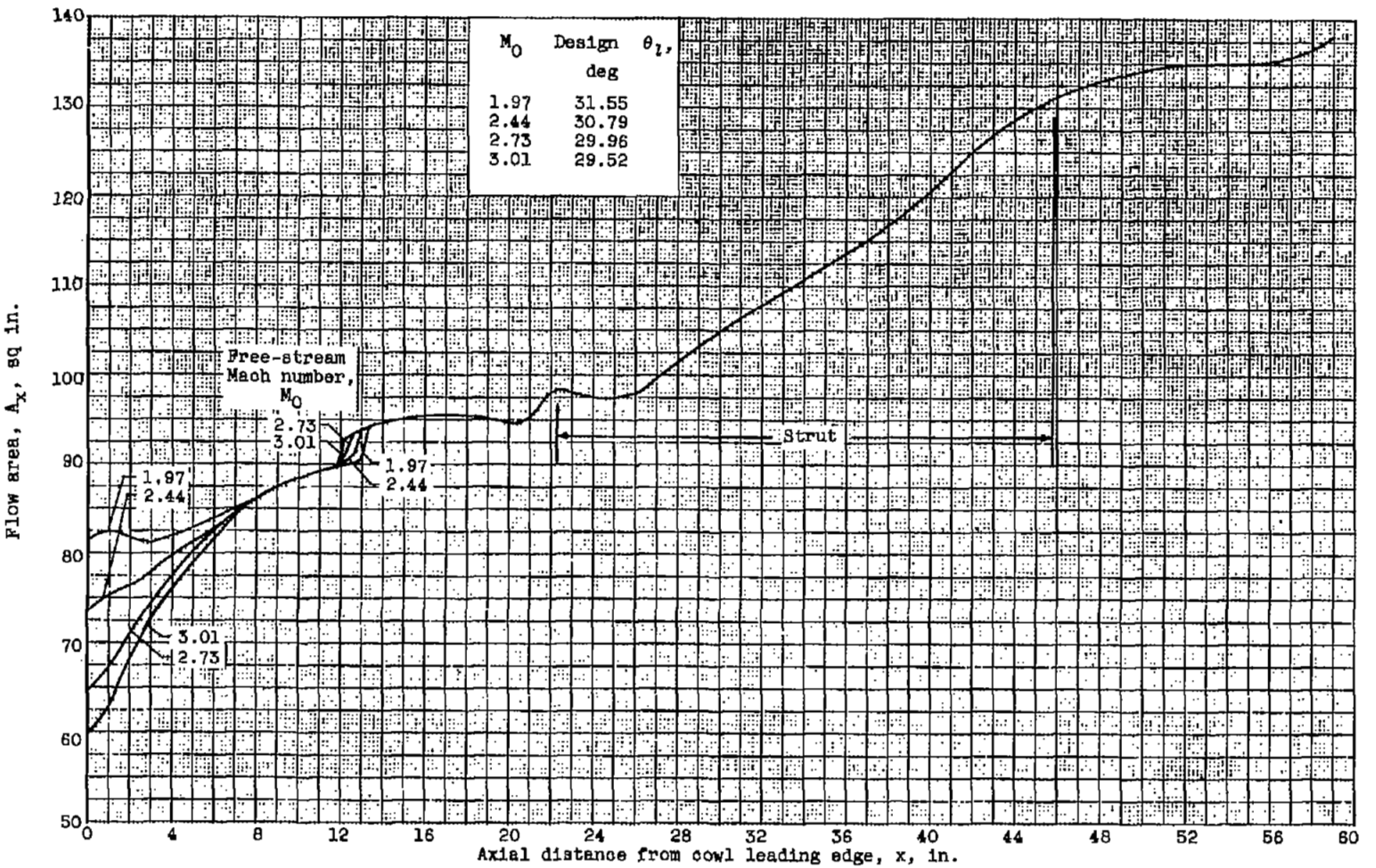

(a) Inlet with 40-percent cowl.

Figure 2. - Internal area distributions for subsonic diffuser at design cowl-position parameter θ_l.

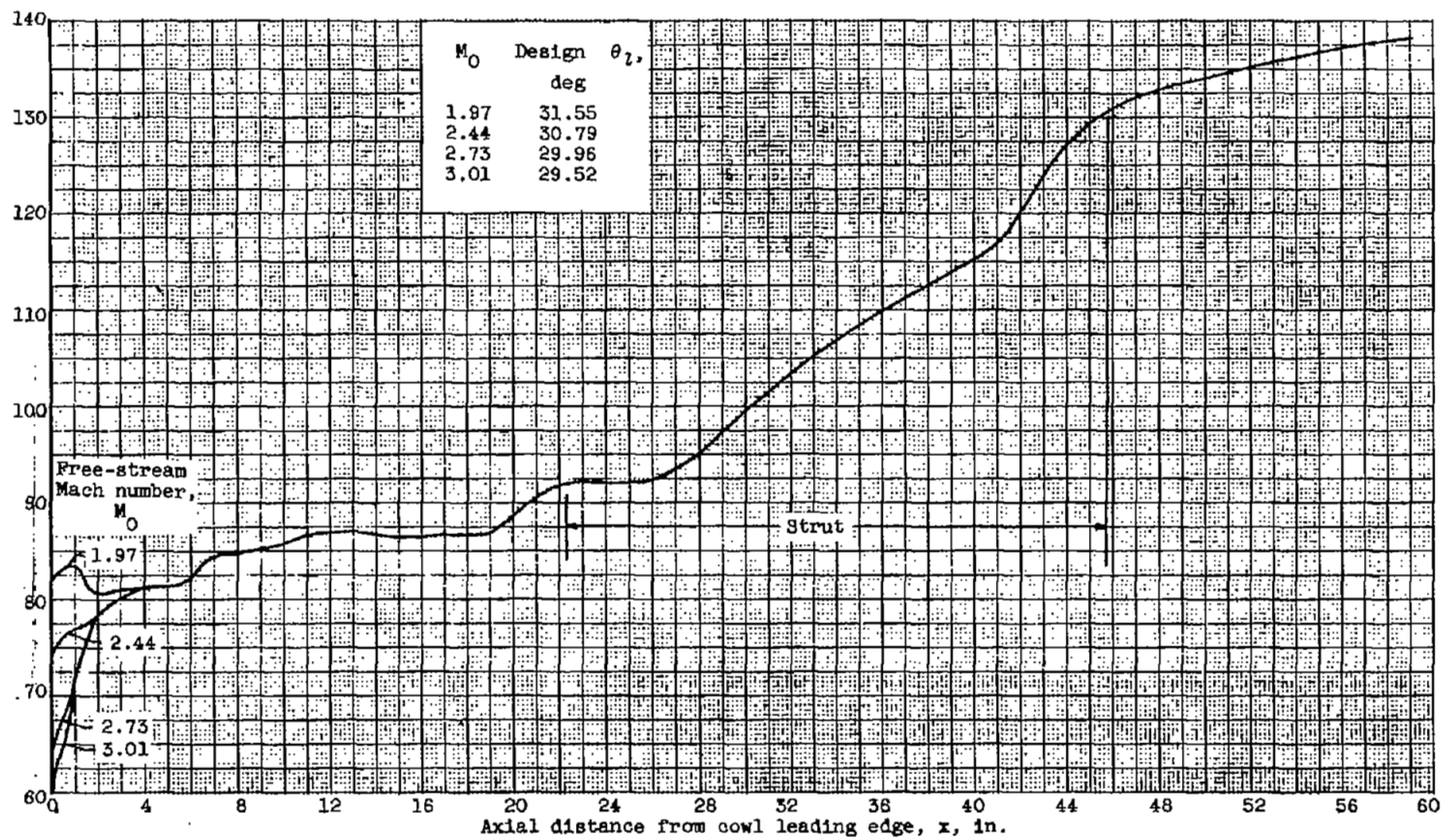

(b) Inlet with 20-percent cowl.

Figure 2. - Concluded. Internal area distributions for subsonic diffuser at design cowl-position parameter θ_l.

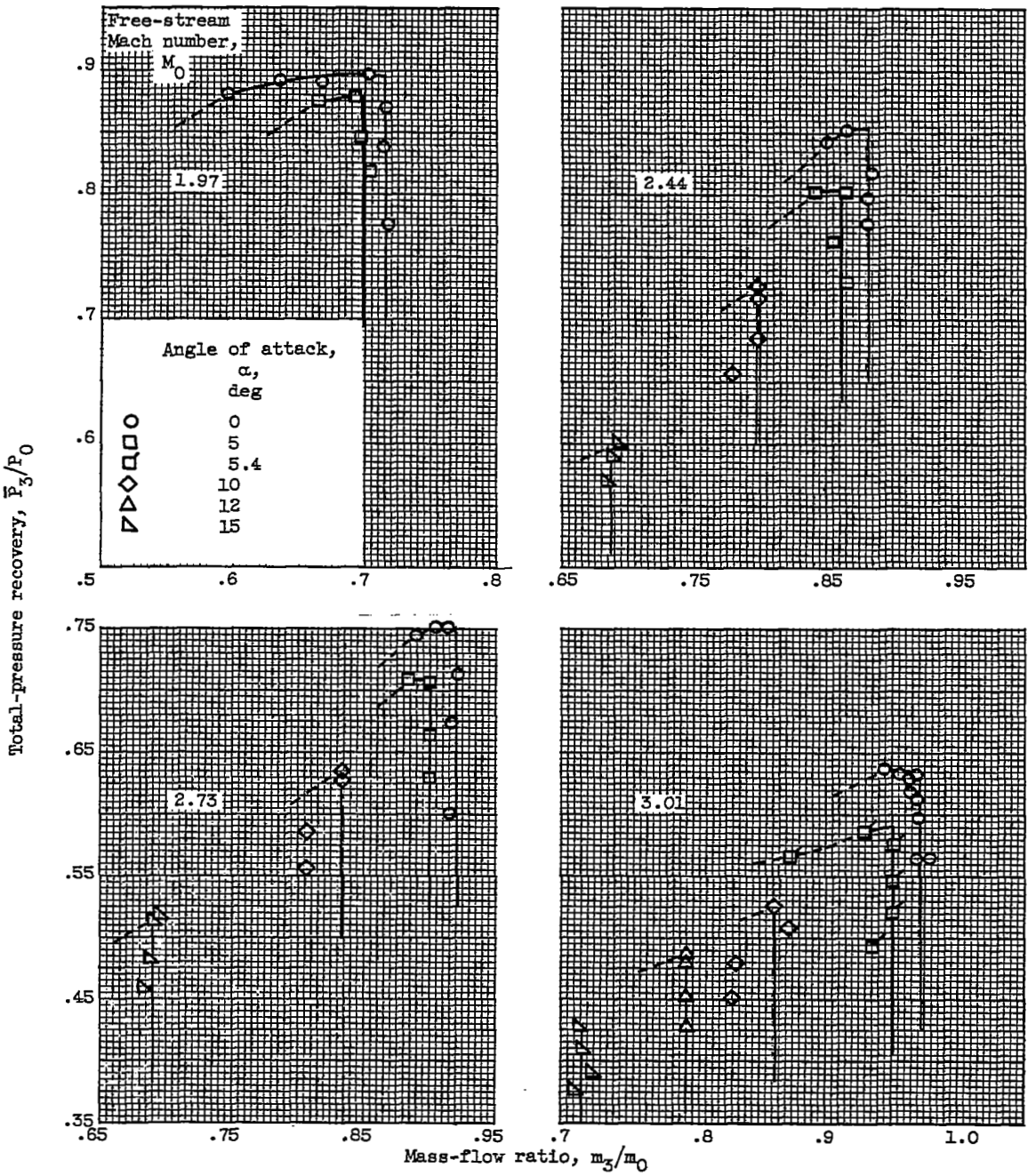

(a) 40-Percent-cowl inlet.

Figure 3. - Diffuser performance characteristics at design cowl-position parameter for each Mach number.

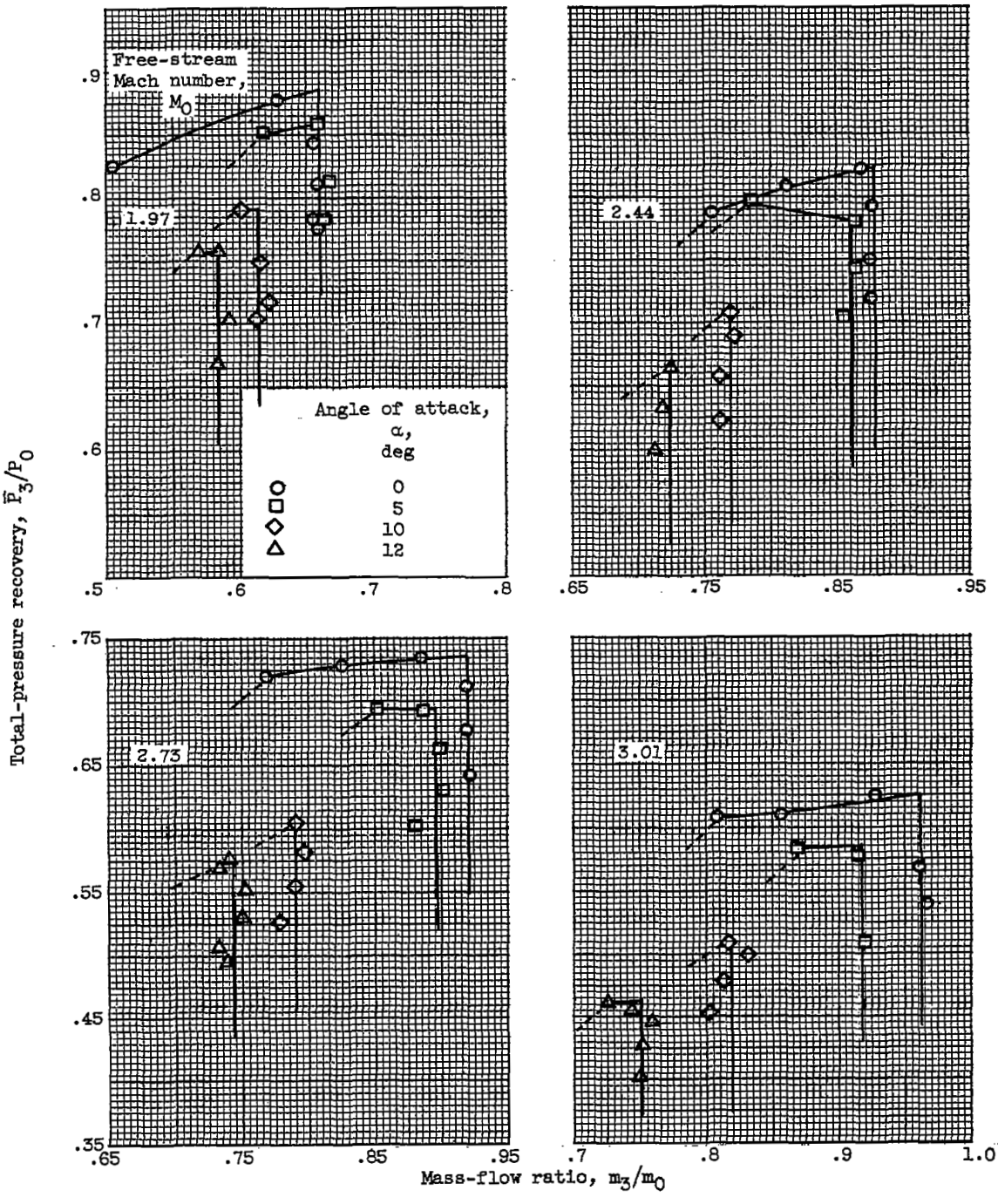

(b) 20-Percent-cowl inlet.

Figure 3. - Concluded. Diffuser performance characteristics at design cowl-position parameter for each Mach number.

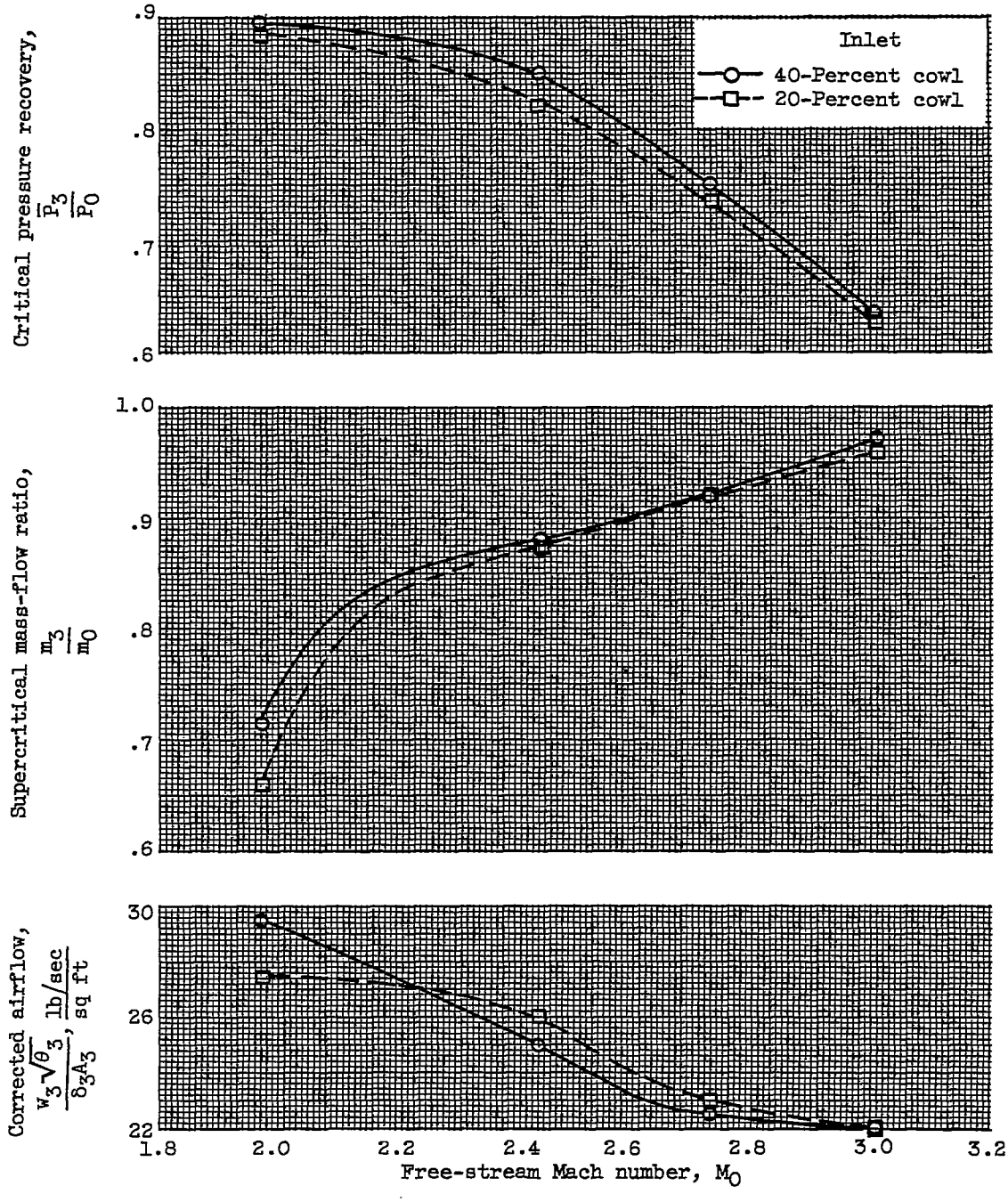

Figure 4. - Variation of critical inlet performance with free-stream Mach number.

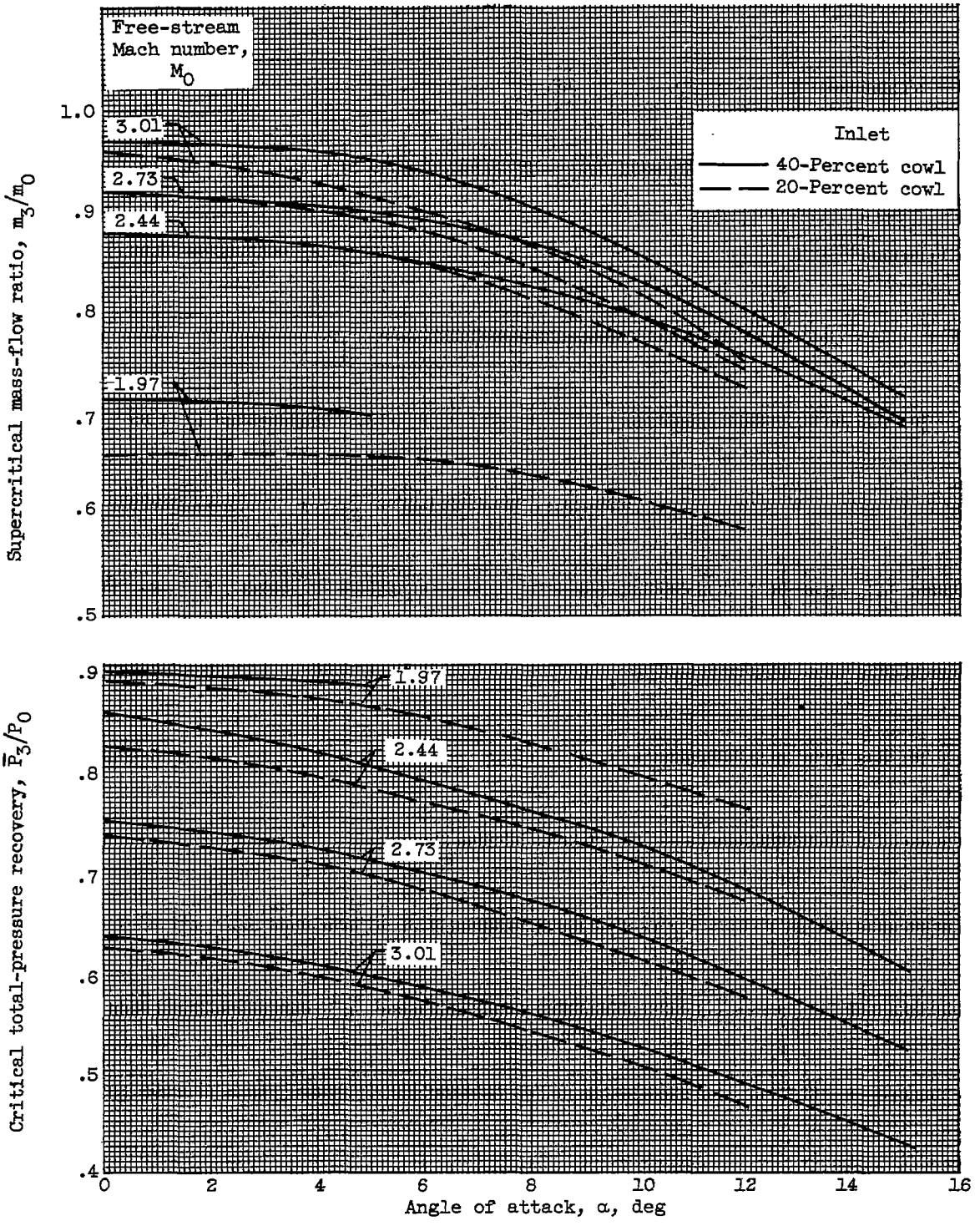

4405

Figure 5. - Effect of angle of attack on internal performance.

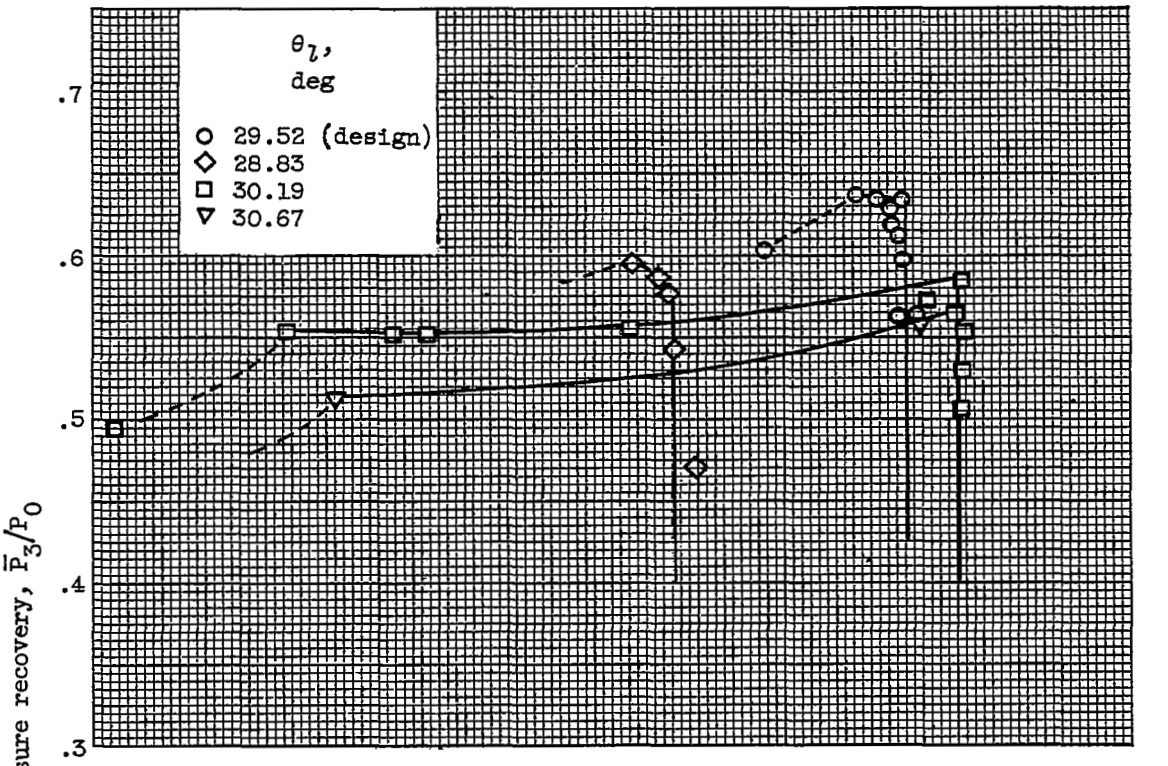

(a) 40-Percent-cowl inlet.

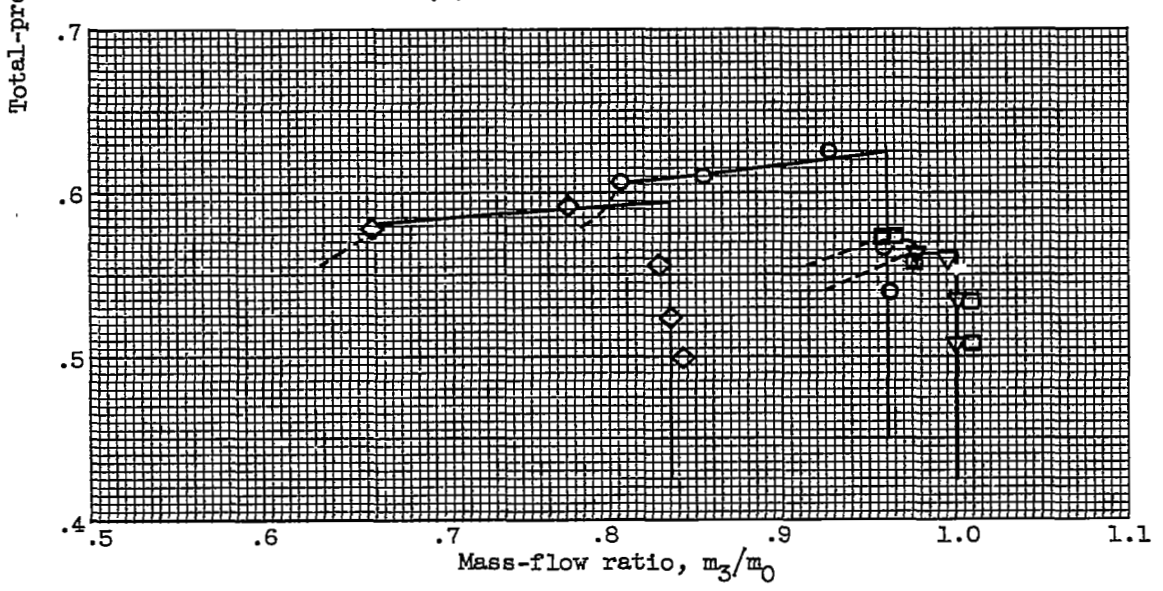

(b) 20-Percent-cowl inlet.

Figure 6. - Diffuser performance characteristics for several values of cowl-position parameter θ_l. Free-stream Mach number, 3.01; angle of attack, 0°.

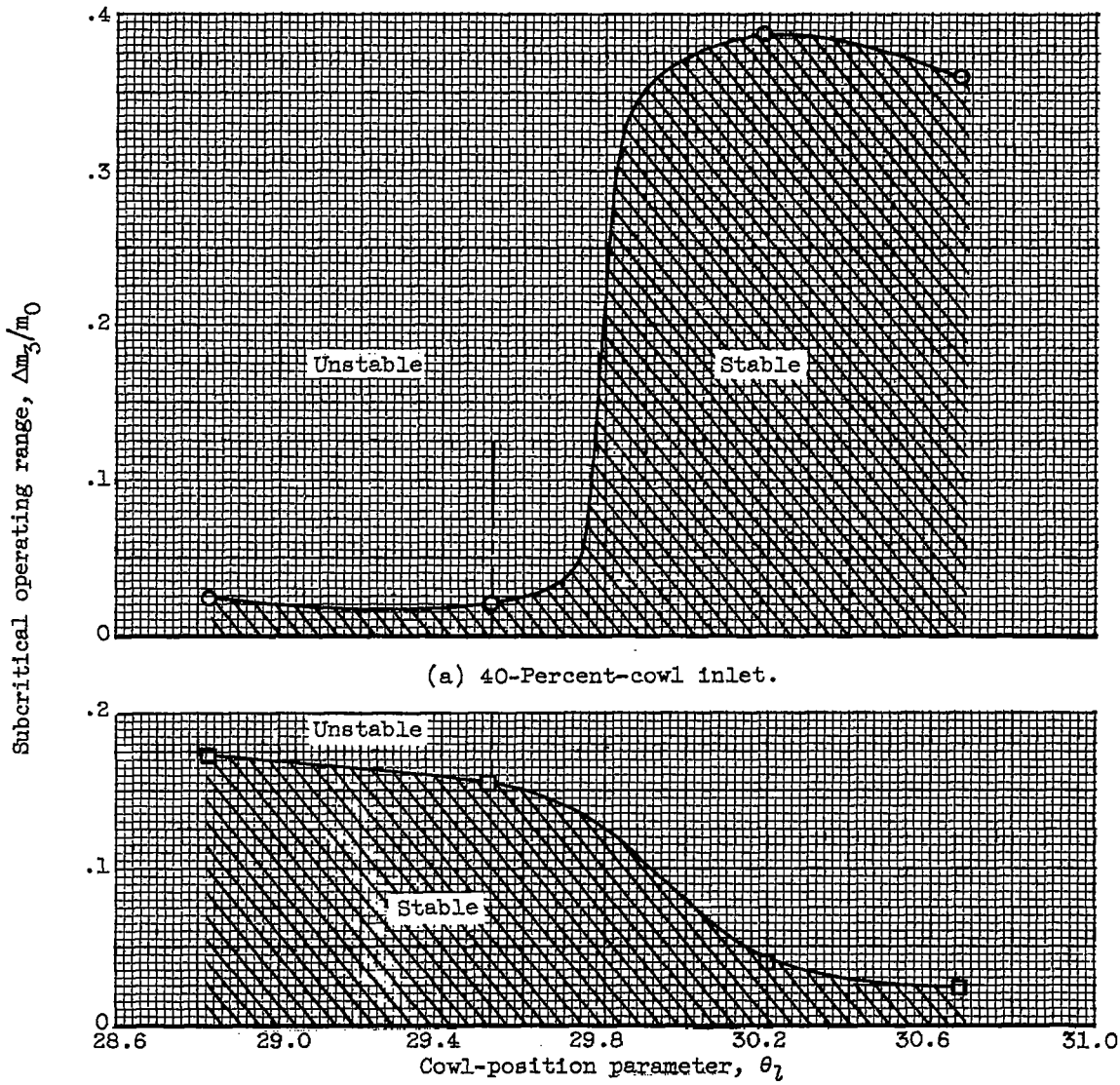

Figure 7. - Effect of spike translation on inlet stability range. Free-stream Mach number, 3.01; angle of attack, 0°.

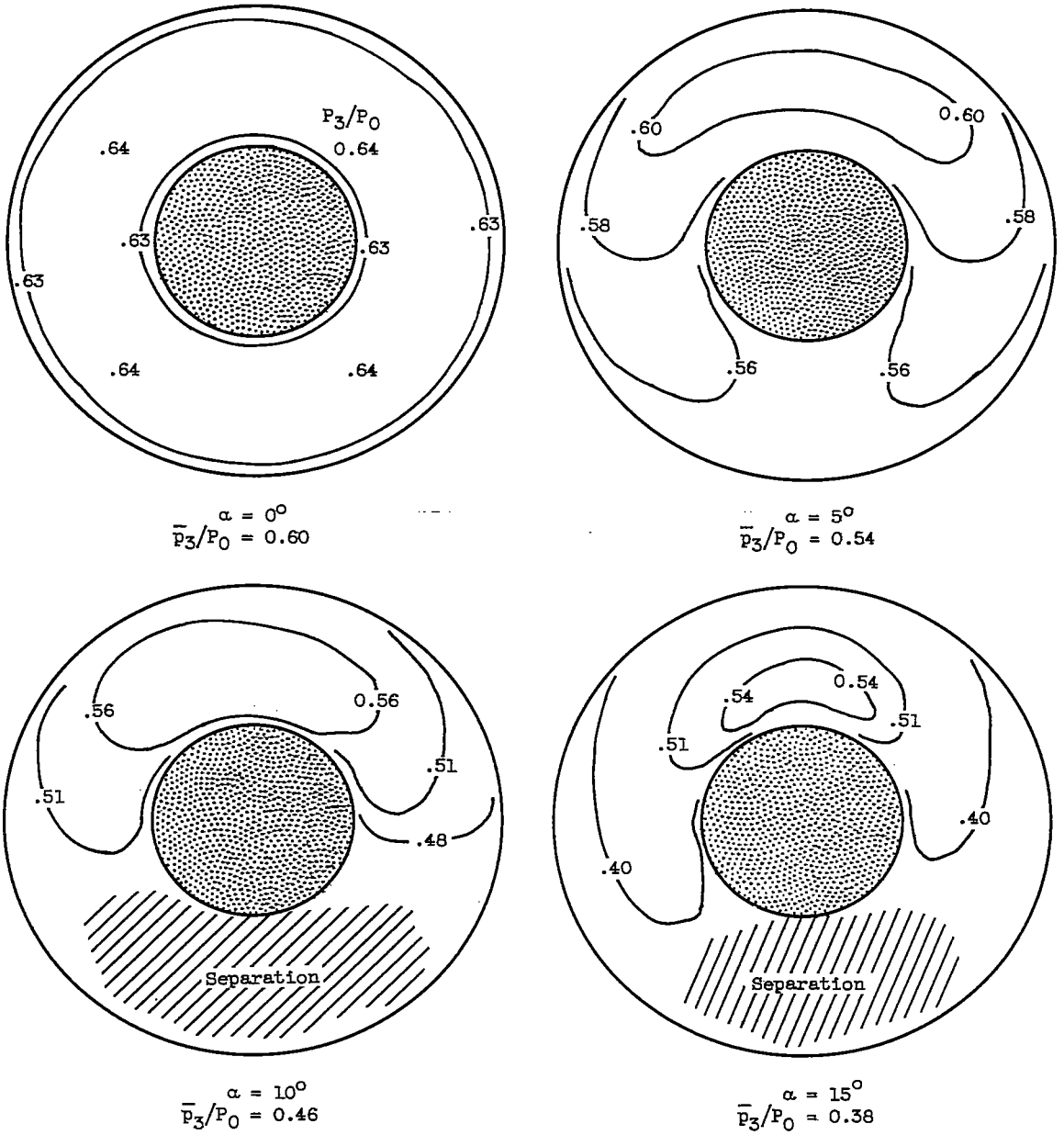

(a) 40-Percent-cowl inlet.

Figure 8. - Total-pressure contours at diffuser exit for near-critical inlet operation. Free-stream Mach number, 3.01.

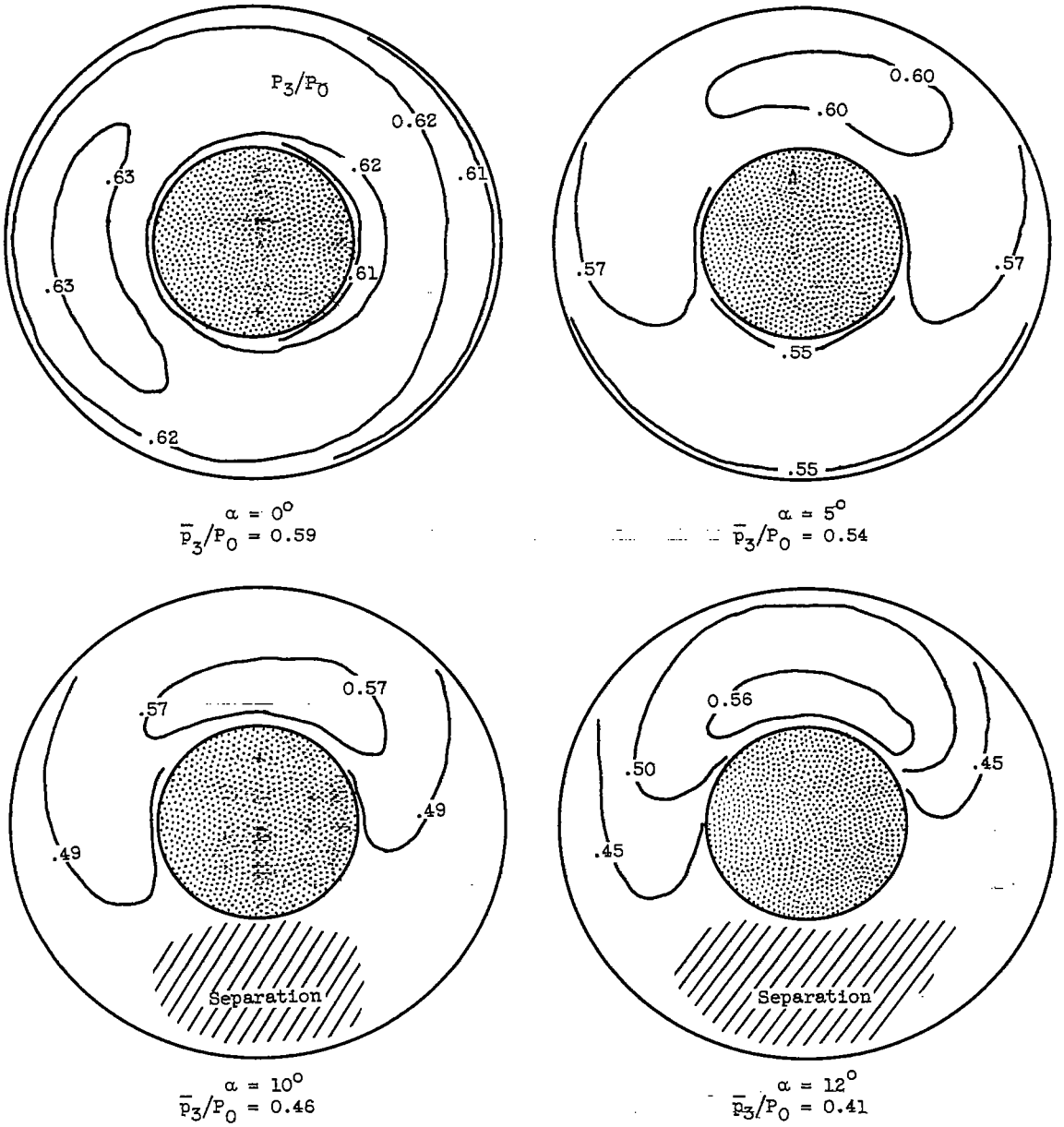

$\alpha = 0^\circ$, $\bar{p}_3/P_0 = 0.59$

$\alpha = 5^\circ$, $\bar{p}_3/P_0 = 0.54$

$\alpha = 10^\circ$, $\bar{p}_3/P_0 = 0.46$

$\alpha = 12^\circ$, $\bar{p}_3/P_0 = 0.41$

(b) 20-Percent-cowl inlet.

Figure 8. - Concluded. Total-pressure contours at diffuser exit for near-critical inlet operation. Free-stream Mach number, 3.01.

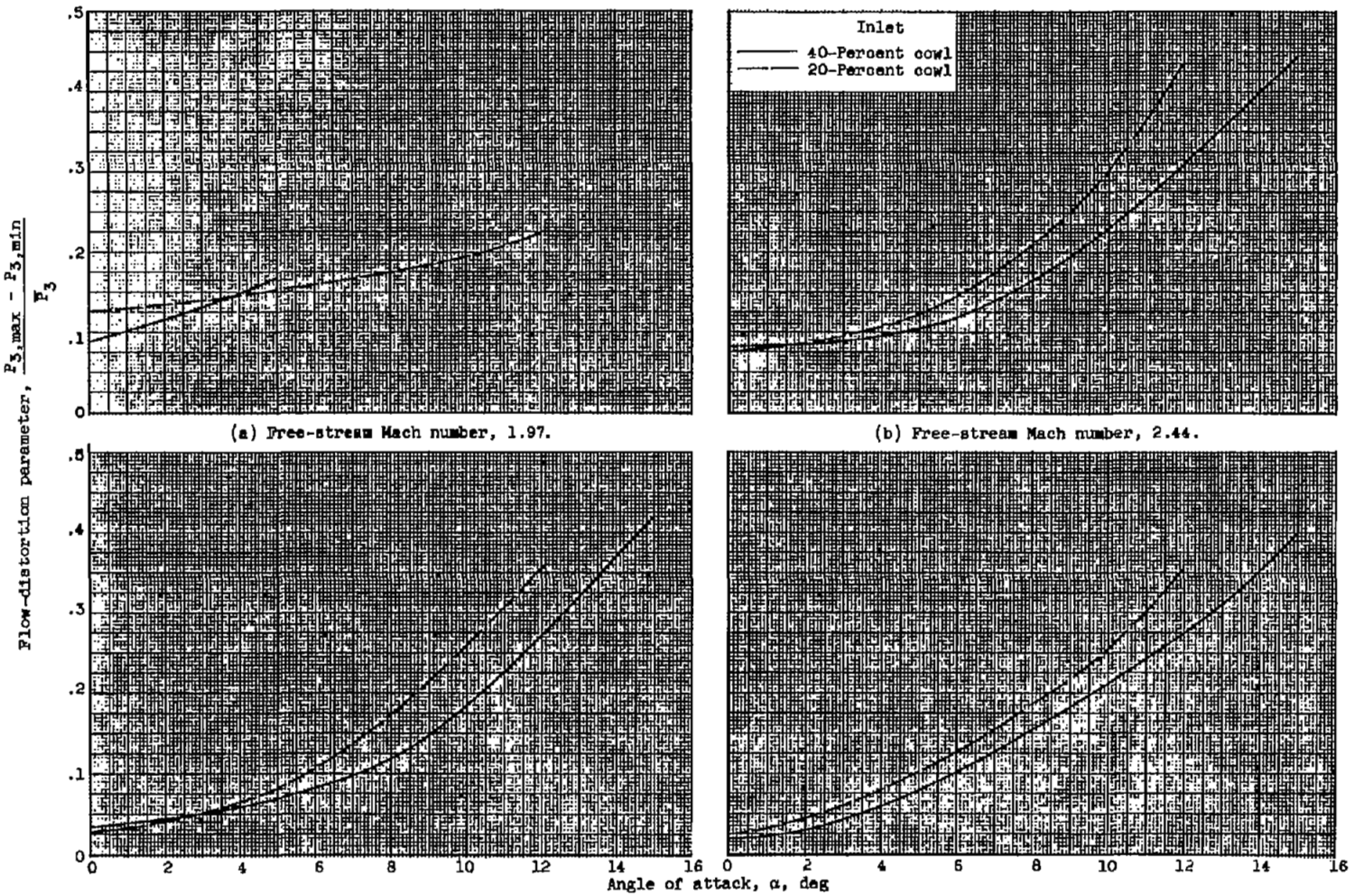

(a) Free-stream Mach number, 1.97.

(b) Free-stream Mach number, 2.44.

(c) Free-stream Mach number, 2.73.

(d) Free-stream Mach number, 3.01.

Figure 9. - Effect of angle of attack on distortion during critical inlet operation.

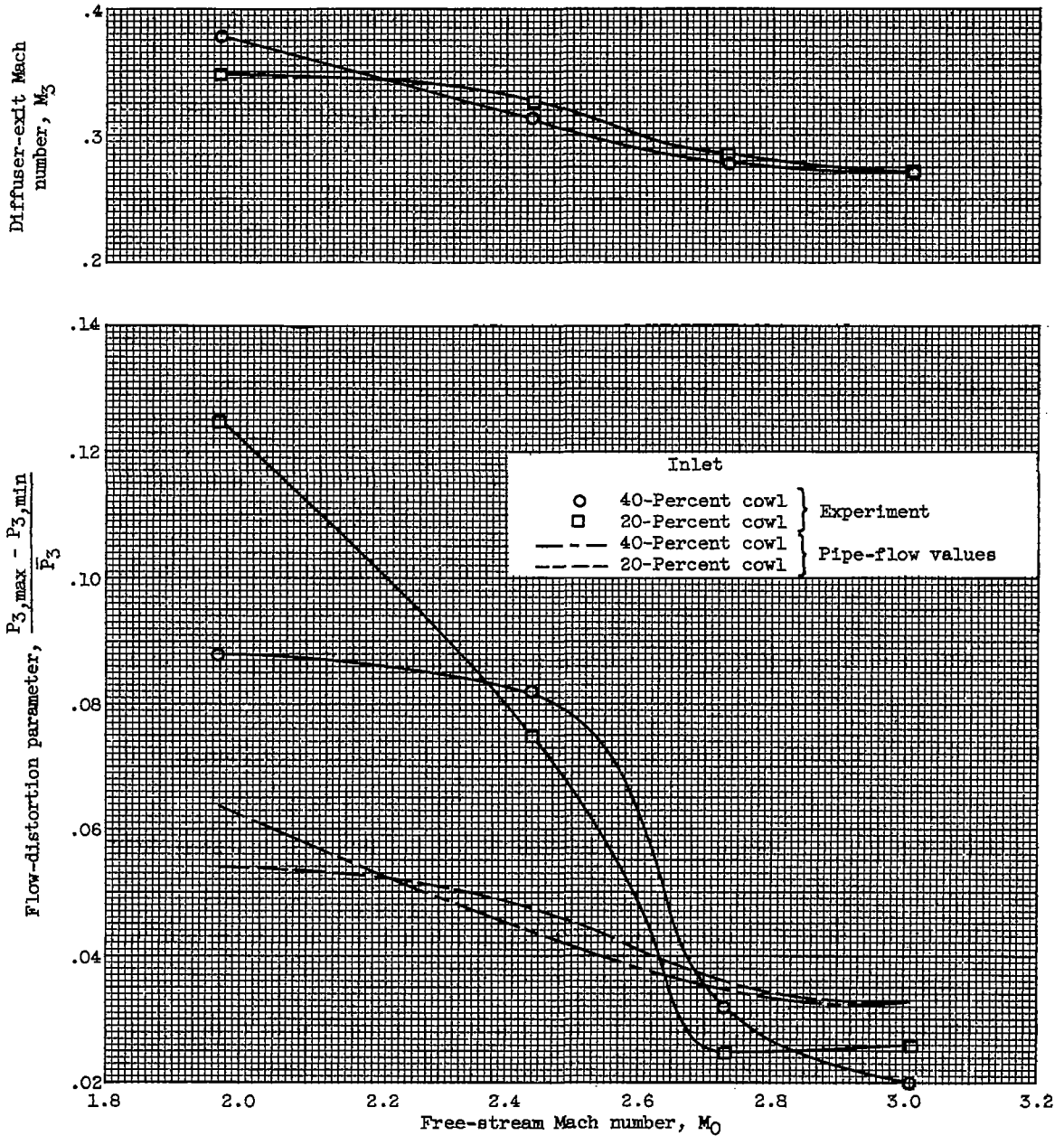

Figure 10. - Comparison of distortion at diffuser exit with theoretical pipe-flow values. Angle of attack, 0°.

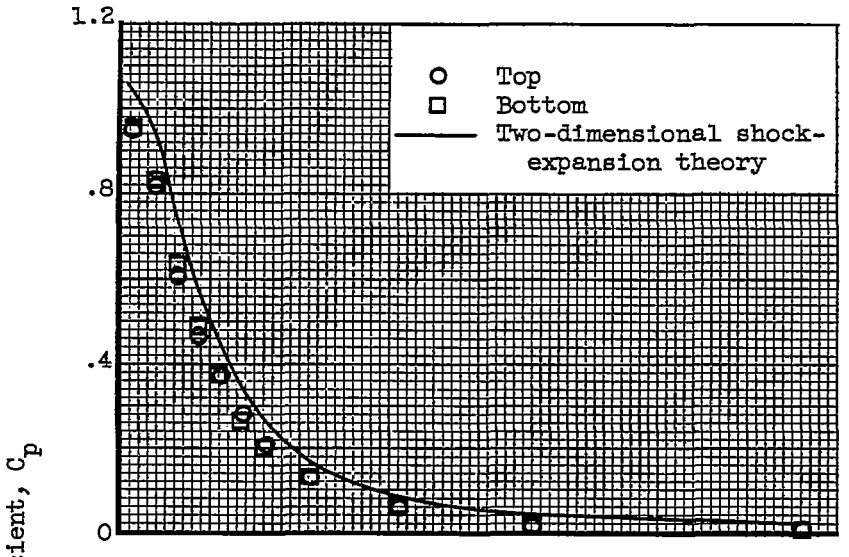

(a) 40-Percent-cowl inlet.

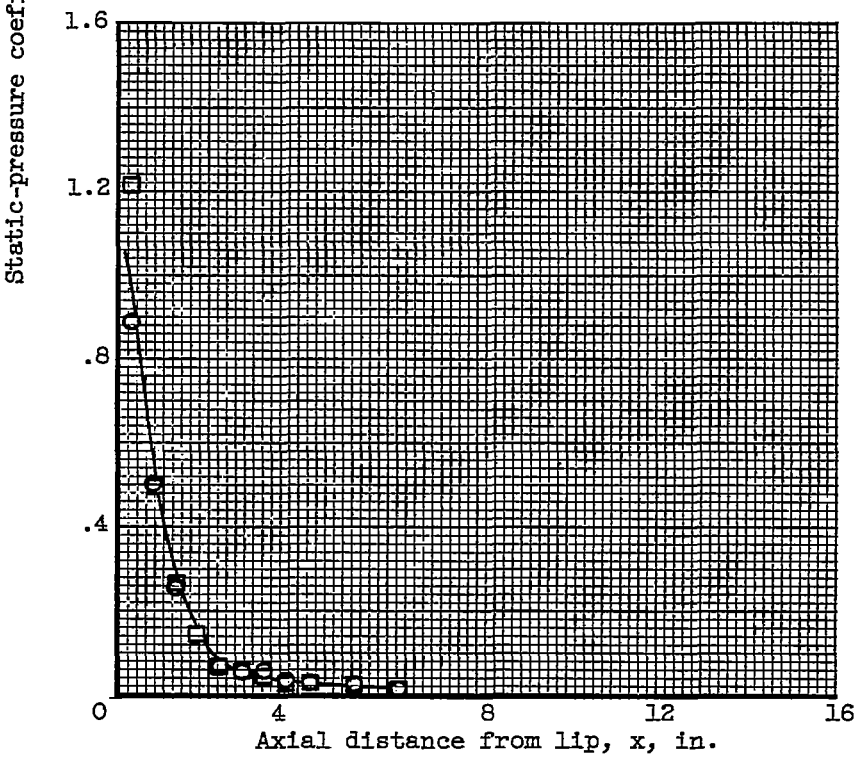

(b) 20-Percent-cowl inlet.

Figure 11. - External static-pressure distributions on cowl. Free-stream Mach number, 3.01; angle of attack, 0°.

[redacted]

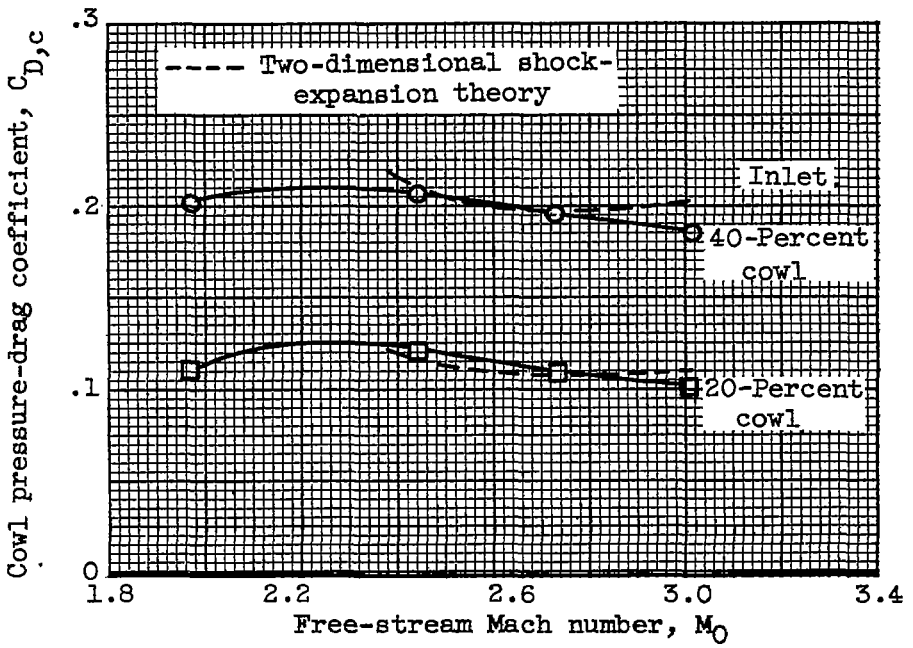

Figure 12. - Cowl pressure drag during supercritical inlet operation at zero angle of attack.

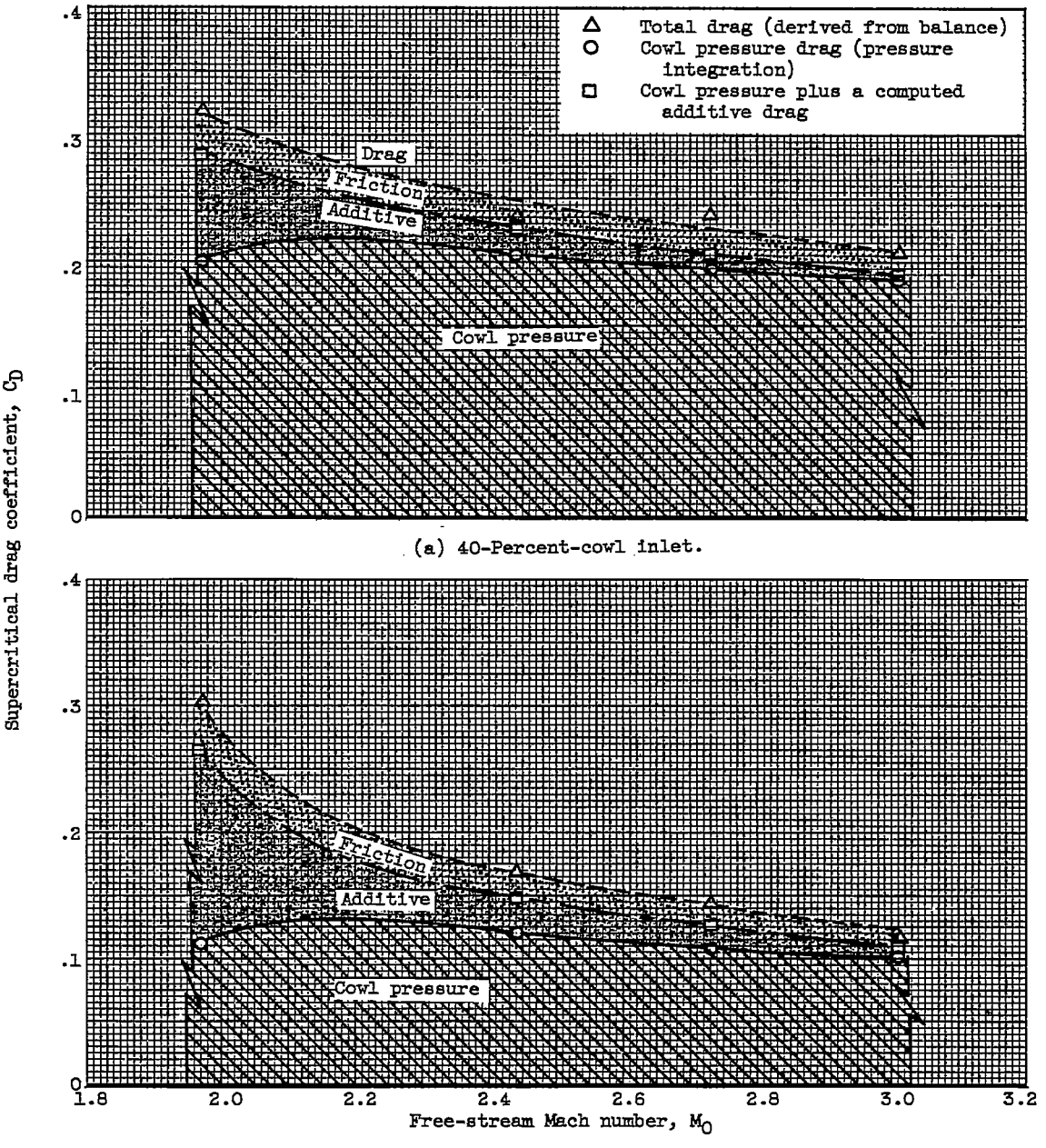

(a) 40-Percent-cowl inlet.

(b) 20-Percent-cowl inlet.

Figure 13. - Component drags during supercritical inlet operation at design cowl-position parameter.

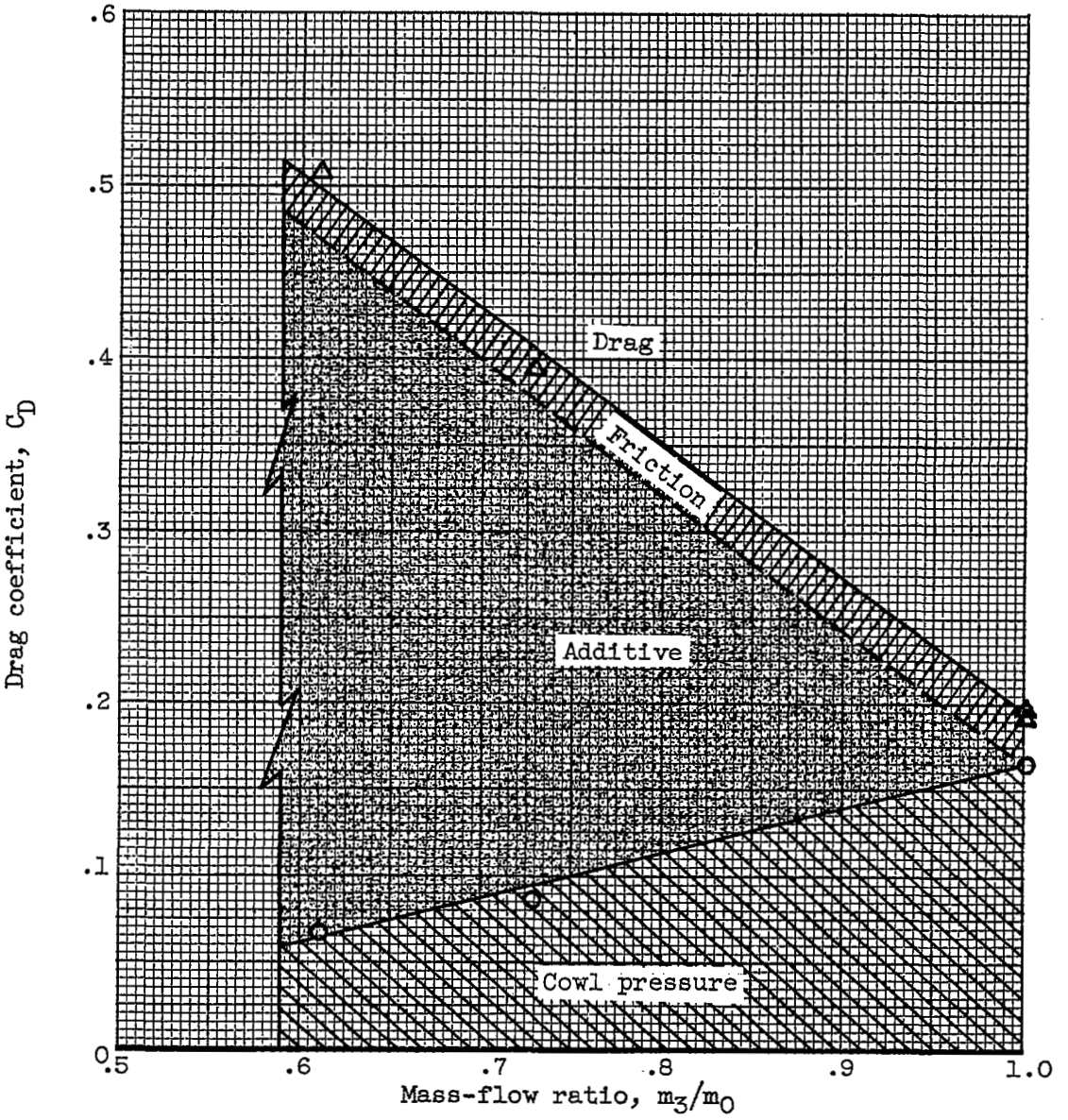

Figure 14. - Component drags for subcritical operation of 40-percent-cowl inlet. Free-stream Mach number, 3.01; cowl-position parameter, 30.19°.

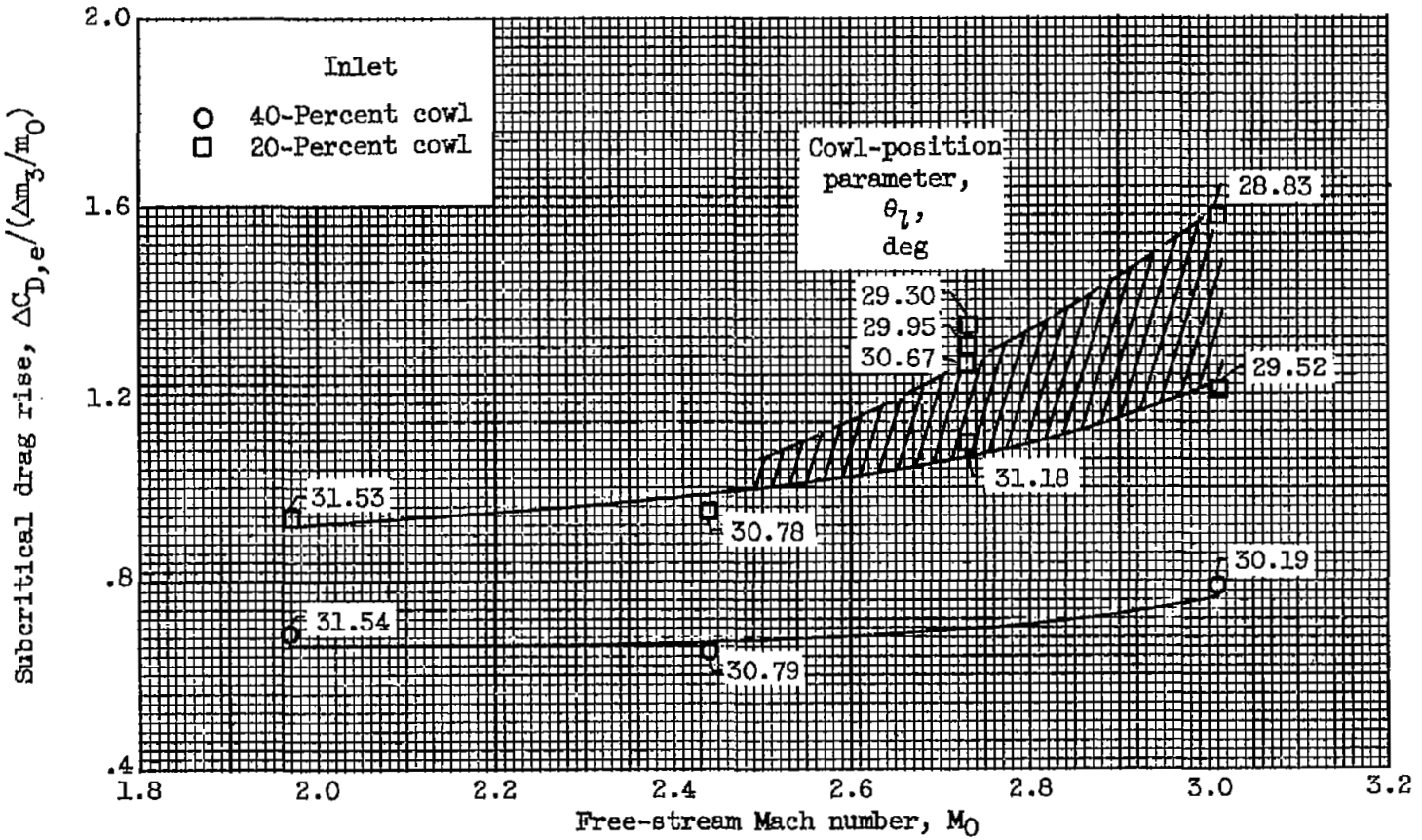

Figure 15. - Rates of increase in subcritical total external drag.

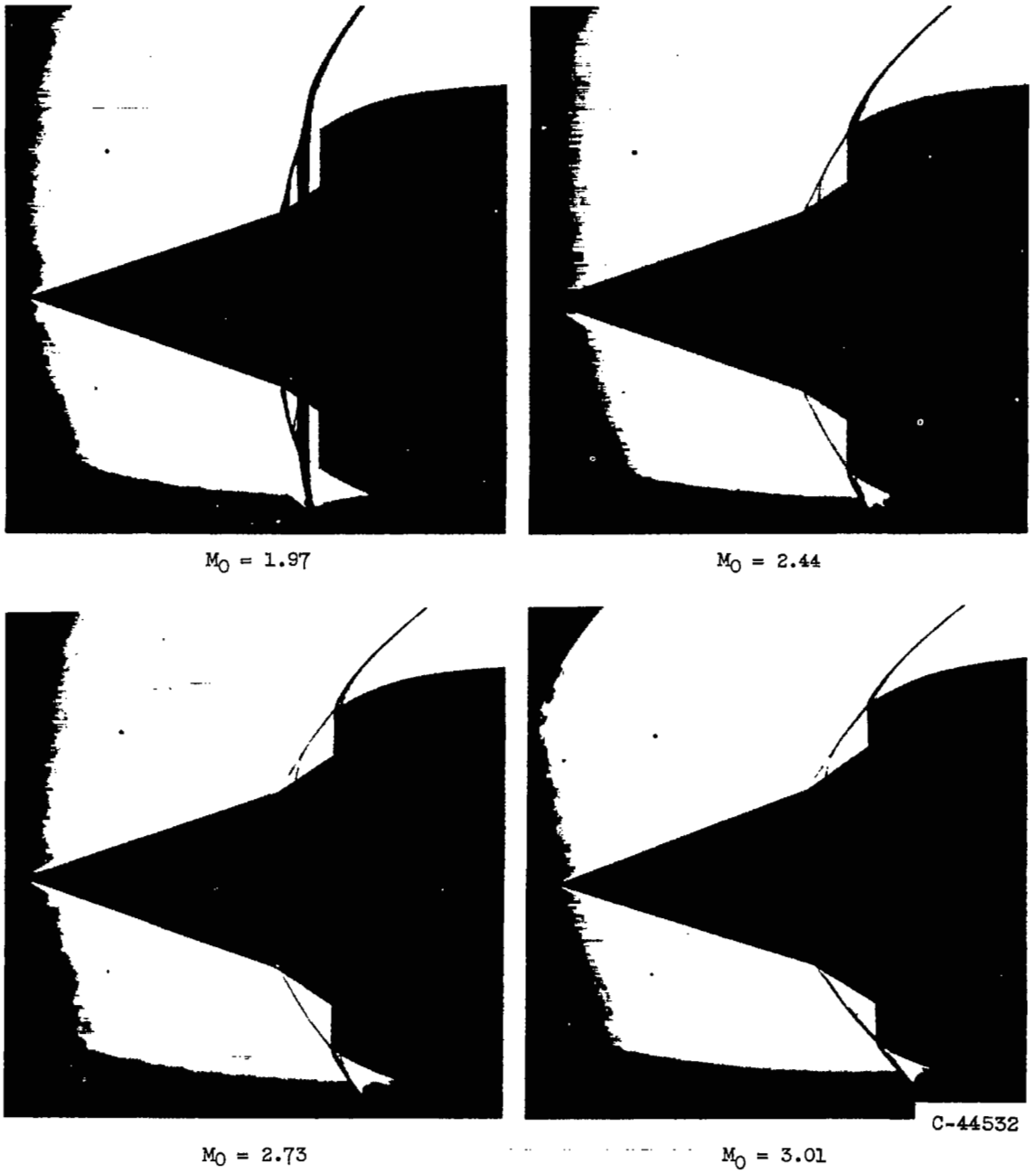

(a) 40-Percent-cowl inlet.

Figure 16. - Flow patterns at several Mach numbers and zero angle of attack.

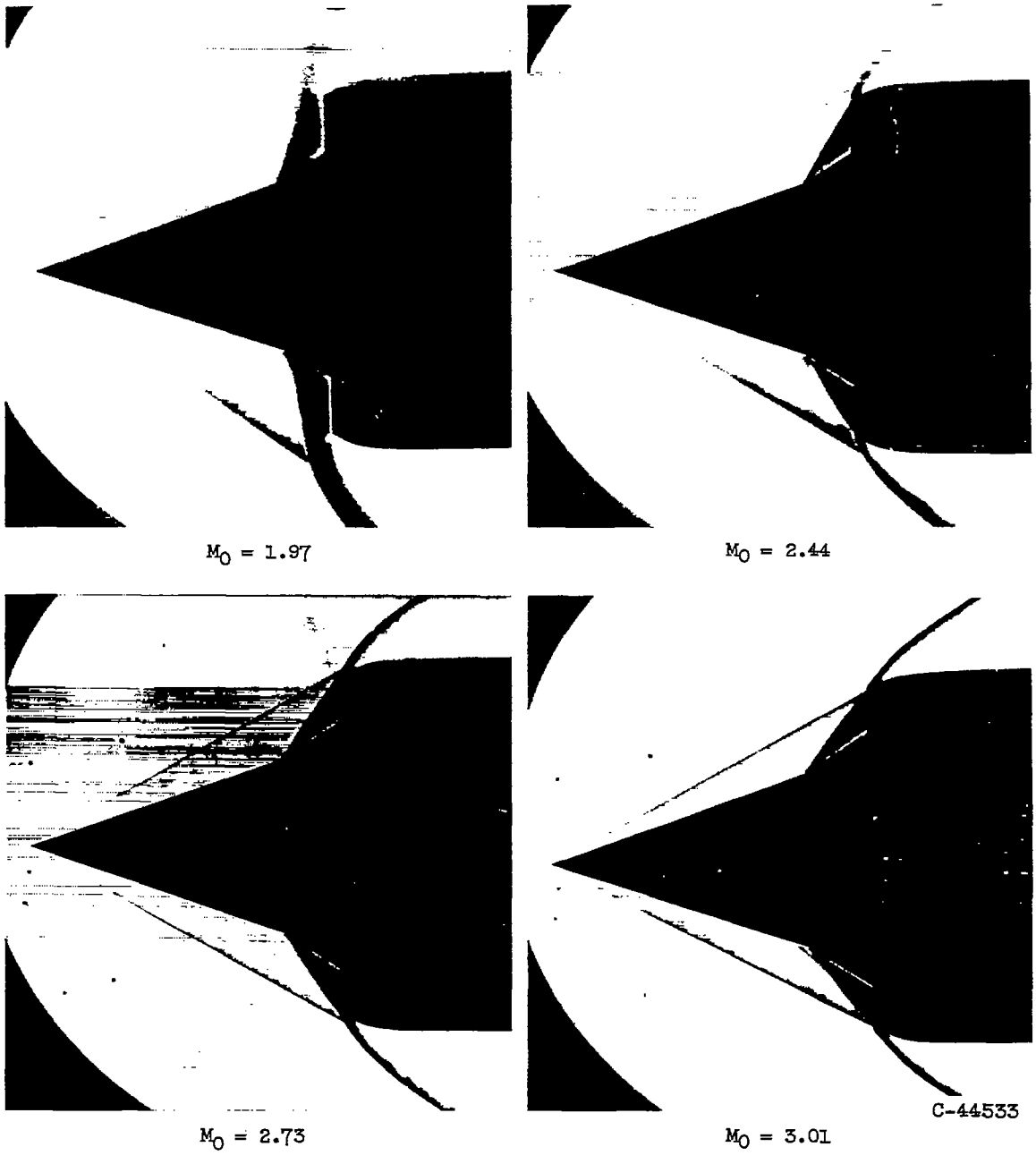

(b) 20-Percent-cowl inlet.

Figure 16. - Concluded. Flow patterns at several Mach numbers and zero angle of attack.

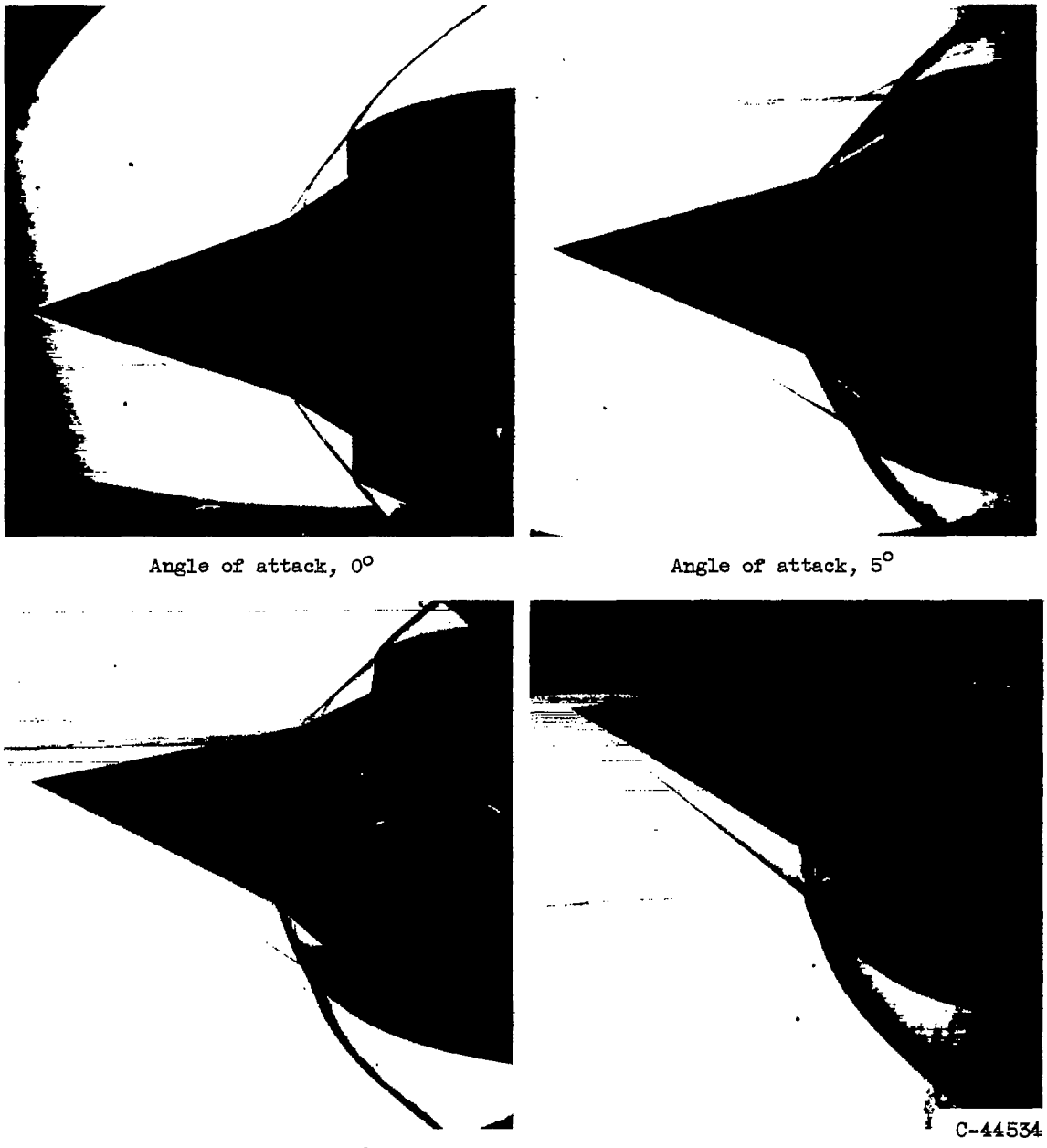

Angle of attack, 0°

Angle of attack, 5°

Angle of attack, 10°

Angle of attack, 15°

(a) 40-Percent-cowl inlet.

Figure 17. - Flow patterns at several angles of attack at Mach number 3.01.

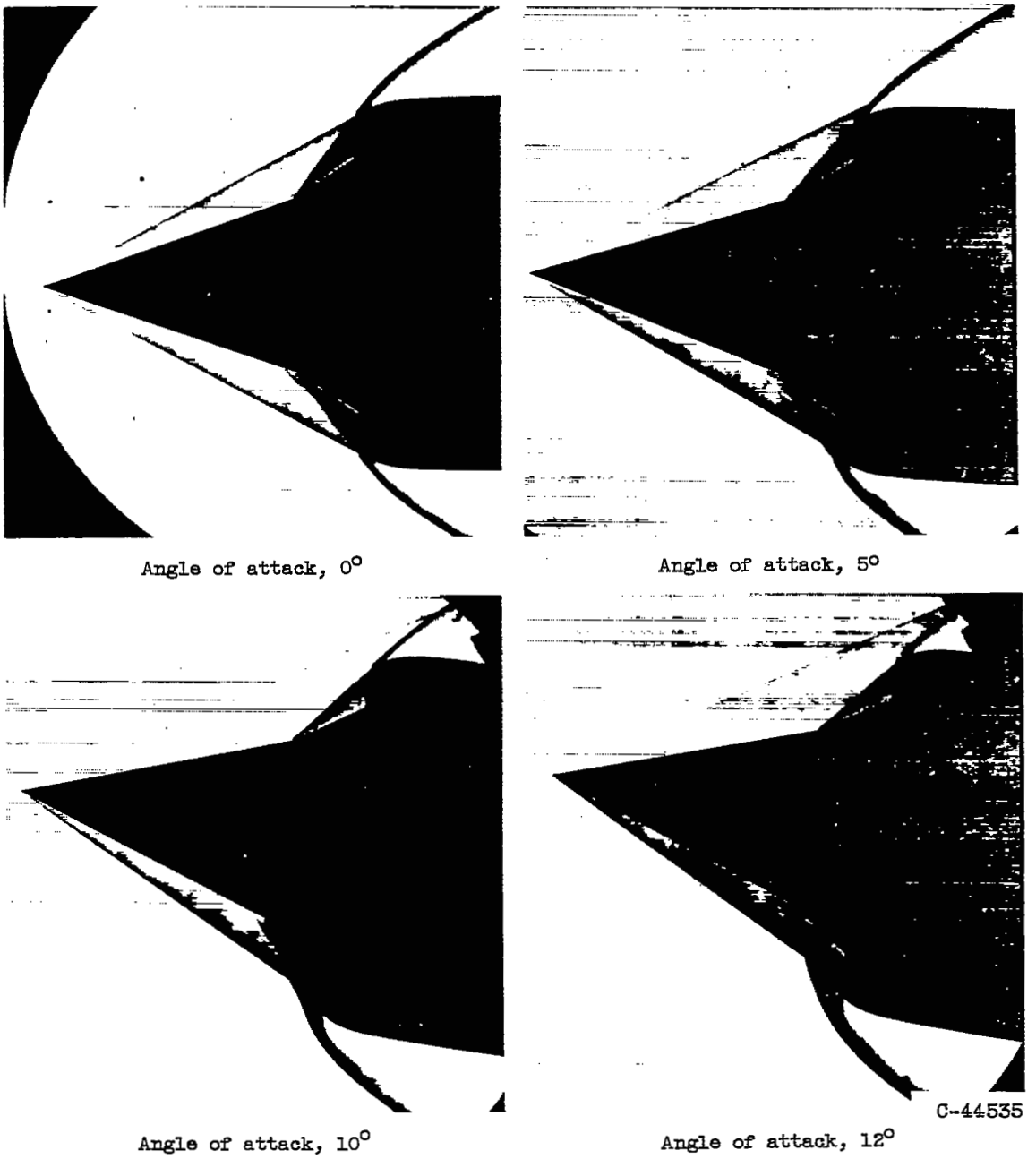

(b) 20-Percent-cowl inlet.

Figure 17. - Concluded. Flow patterns at several angles of attack at Mach number 3.01.

C-44536

Supercritical operation

Minimum stable operation

Figure 18. - Supercritical and minimum stable subcritical flow patterns with 40-percent-cowl inlet. Free-stream Mach number, 3.01; cowl-position parameter greater than design.

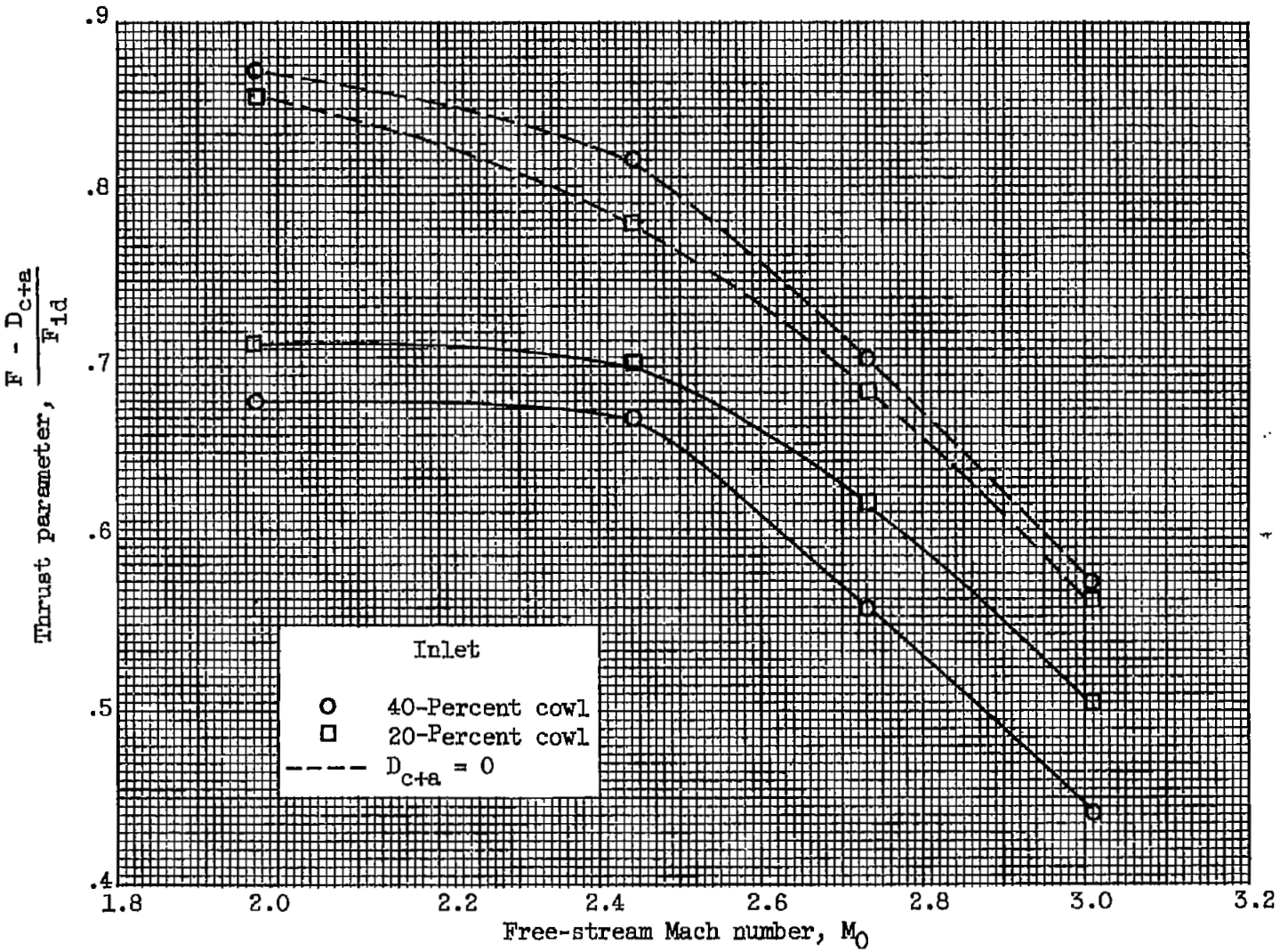

Figure 19. - Propulsive-thrust comparison of performance of 40- and 20-percent-cowl inlets.

[redacted]

NOTES: (1) Reynolds number is based on the diameter of a circle with the same area as that of the capture area of the inlet.

(2) The symbol * denotes the occurrence of buzz.

REPORT AND FACILITY	DESCRIPTION: CONFIGURATION	DESCRIPTION: NUMBER OF OBLIQUE SHOCKS	DESCRIPTION: TYPE BOUNDARY-LAYER CONTROL	TEST PARAMETERS: MACH NO. M_0	TEST PARAMETERS: Re $\times 10^{-6}$	TEST PARAMETERS: ANGLE OF ATTACK α	TEST PARAMETERS: ANGLE OF YAW ψ	TEST DATA: DRAG	TEST DATA: INLET FLOW PROFILE	TEST DATA: DISCHARGE FLOW PROFILE	TEST DATA: FLOW PICTURE	PERFORMANCE: MAX. TOTAL PRESS. RECOV. P/P_0	PERFORMANCE: MASS FLOW RATIO m/m_0	REMARKS
CONFID. RM E57C06 Lewis 10- by 10-ft unitary wind tunnel	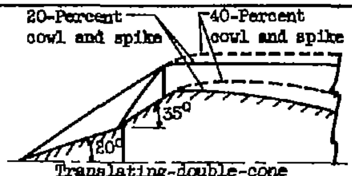 Translating-double-cone axisymmetric inlets	2	None	3.01 2.73 2.44 1.97	3.07 3.07 3.07 3.07	0° to 15°	0 0 0 0	√ √ √ √		√ √ √ √	√ √ √ √	0.635 .75 .85 .895	1 to 0.5*	Essentially no difference in internal performance between two inlets having contrasting rates of turning at the shoulder. The 45-percent-lower cowl drag of the 20-percent-cowl inlet made it superior over entire range.
CONFID. RM E57C06 Lewis 10- by 10-ft unitary wind tunnel	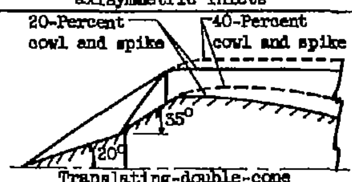 Translating-double-cone axisymmetric inlets	2	None	3.01 2.73 2.44 1.97	3.07 3.07 3.07 3.07	0° to 15°	0 0 0 0	√ √ √ √		√ √ √ √	√ √ √ √	0.635 .75 .85 .895	1 to 0.5*	Essentially no difference in internal performance between two inlets having contrasting rates of turning at the shoulder. The 45-percent-lower cowl drag of the 20-percent-cowl inlet made it superior over entire range.
CONFID. RM E57C06 Lewis 10- by 10-ft unitary wind tunnel	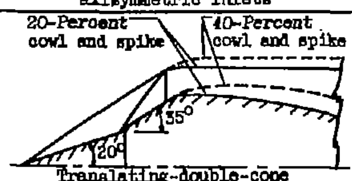 Translating-double-cone axisymmetric inlets	2	None	3.01 2.73 2.44 1.97	3.07 3.07 3.07 3.07	0° to 15°	0 0 0 0	√ √ √ √		√ √ √ √	√ √ √ √	0.635 .75 .85 .895	1 to 0.5*	Essentially no difference in internal performance between two inlets having contrasting rates of turning at the shoulder. The 45-percent-lower cowl drag of the 20-percent-cowl inlet made it superior over entire range.